SEDIMENTOLOGY the journal of the International Association of Sedimentologists

*Sedimentology* (2016) **63**, 1209–1232 doi: 10.1111/sed.12257

# Porosity and size gradation of saturated gravel with percolated fines

FRANCISCO NÚÑEZ-GONZÁLEZ*,[1], JUAN PEDRO MARTÍN-VIDE† and MAARTEN G. KLEINHANS‡

**Department of Water and Waste Management, University of Applied Sciences Magdeburg-Stendal, Breitscheidstr. 2, 39114 Magdeburg, Germany (E-mail: f.nunez-gonzalez@tu-braunschweig.de)*

*†Hydraulics Department Technical University of Catalonia (BarcelonaTech), Barcelona, Spain*

*‡Faculty of Geosciences, Utrecht University, The Netherlands*

Associate Editor – Subhasish Dey

**ABSTRACT**

Fine particles may infiltrate through coarse alluvial beds and eventually saturate the subsurface pore space. It is essential to understand the conditions that lead to bed saturation, and to forecast the packing characteristics of saturated beds to assess the effect of excess fine sediment supply on a number of processes that occur in the stream–sediment boundary. To address this problem, in this study, a new method is introduced to predict the grain-size distribution for the saturated condition, and the resulting porosity decrease, given the characteristics of the bed and the supplied sediments. The new method consists of the numerical aggregation of infilling fines in a finite bed volume, during which the bed properties change to affect further infilling. An existing semi-empirical, particle packing model is implemented to identify these properties. It is shown that these types of models are adequate to describe regimes of natural sediment fabric quantitatively, and are thus useful tools in the analysis of sediment infiltration processes. Unlike previous developments to quantify saturated bed conditions, which assume that the supplied material is uniform and finer than the bed pore openings, the method developed herein considers poorly sorted fines, and can identify size fractions that are able to ingress into the bed due to being smaller than the particles that form the bed structure. Application of the new method to published experimental data showed that the final content of infiltrated fines is strongly sensitive to the initial bed packing density, highlighting the need to measure and understand open-work gravel deposits. In addition, the new method was shown to be suitable for assessing the degree of bed saturation, when it was applied to a published data set of field samples.

**Keywords** Clogging, colmation, infiltration, porosity, sediment mixtures, siltation.

## INTRODUCTION

Infiltration of fine particles in gravel beds might lead to saturation of the pore space, i.e. the almost complete occupation of the pores by fine material. This process, which is also known as clogging or colmation, reduces bed permeability and porosity (Schälchli, 1992; Wu & Huang, 2000), and has adverse effects for the survival of salmonid alevins (Peterson, 1978; Chapman,

[1]Present address: Leichtweiß-Institute for Hydraulic Engineering, Department for Hydraulic Engineering, Technische Universität Braunschweig, Beethovenstr. 51a, 38106 Braunschweig, Germany.

1988) and organisms in the hyporheic zone (Brunke, 1999; Rehg *et al.*, 2005). In consequence, the degree of bed saturation with fines may be indicative of the health of a stream ecosystem (Gayraud & Philippe, 2003; Coulombe-Pontbrianda & Lapointe, 2004; Julien & Bergeron, 2006; Denic & Geist, 2015). Bed saturation also has an effect on stream bed morphodynamics: the infilling of superficial pores with fine material makes the bed surface smoother, and modifies the mobility of the particles (Iseya & Ikeda, 1987; Wilcock & Kenworthy, 2002; Sambrook Smith & Nicholas, 2005). In addition, superficial saturation prevents further percolation of fines deposited on the bed surface. Thus, saturation sets a limit from which fine particles do not occupy the pore space after sedimentation, but effectively contribute to morphological changes (Frings *et al.*, 2008).

Saturation with fines can occur in shallow or deep bed layers. It occurs near the bed surface when the size of the infiltrated material is not much smaller than the bed pores (Lisle, 1989; Diplas & Parker, 1992); this allows the formation of bridges when two particles fall simultaneously into the same hole and occlude it (Sakthivadivel & Einstein, 1970; Alberts, 2005). A dense deposit of fines might build up above the bridges. When the fine material is much finer than the pores between large particles, a process known as 'unimpeded static percolation' occurs (Kleinhans, 2002; Gibson *et al.*, 2009). For this condition, fine material penetrates down into the bed to an impervious or reduced porosity layer. On this layer, fines build up and fill the bed from the bottom up (Einstein, 1968; Sakthivadivel & Einstein, 1970; Beschta & Jackson, 1979; Gibson *et al.*, 2010), as occurs in an hourglass.

Assessment of the degree of saturation of an alluvial bed is important to understanding of sediment infiltration processes, and their effects on hyporheic ecosystems or on the morphodynamics of gravel bed streams. Notwithstanding, there is little understanding of the conditions that favour saturation when fine material percolates in the bed, driven only by gravitational forces. Different authors have developed theoretical (Sakthivadivel & Einstein, 1970; Lauck, 1991; Cui *et al.*, 2008), numerical (Cui *et al.*, 2008) and empirical (Wooster *et al.*, 2008) models to describe the vertical distribution of percolated fines. Some of these models require an *a priori* definition of the saturation conditions to attain stability. In this regard, Wooster *et al.* (2008) presented a semi-empirical equation to estimate the saturation content of the fine sediment fraction, as a function of the mean diameters and standard deviations of the coarse bed and infiltrated fine materials. In natural streams, the largest proportion of infiltrated sediment is commonly generated from the finest grain-size fractions of the bedload (Lisle, 1989), which is normally composed of a wide assortment of grain sizes. Because the equation of Wooster *et al.* (2008) was developed from experiments with only one type of fine sediment, with a uniform grain-size distribution, this equation cannot be generalized to the most common conditions in natural gravel bed streams.

This study presents a new method for forecasting the relative content of fine sediment as the pore space of a coarse sediment matrix is progressively saturated. The suggested method, which estimates the porosity and grain-size gradation of the saturated bed, consists of integrating numerically the mass conservation equation for fine sediment infiltration in an immobile bed, as developed by Cui *et al.* (2008). Equations are presented that generalize the theory of Cui *et al.* (2008) to any arbitrary number of grain-size fractions. Moreover, to identify the saturation state, a packing porosity model is used, which was originally developed by Yu & Standish (1991) for applications in the chemical industry. The present authors suggest that this type of model could be the basis for describing the structure of natural alluvial beds, and for forecasting the conditions that control saturation with infiltrating fines. In this study, fines are defined as the grain-size fractions that are smaller than the size of the bed pores. To estimate a surrogate of the bed pore size, the new method also uses the packing porosity model of Yu & Standish (1991). The model herein predicts the progressive filling of a volume, such that the conditions for percolation change during the process, depending on the initial conditions, as would occur in nature.

Near-bed turbulence is known to affect the actual degree of saturation as opposed to the maximum degree addressed in this article. Turbulence causes forces on embedded particles through pressure fluctuations, that may cause entrainment of fines out of the pockets between the gravel (Carling, 1984; Vollmer & Kleinhans, 2007). On the other hand, the addition of fines may also lead to a mortaring effect that strengthens the entire bed (Hodge *et al.*, 2013). For the development of forecasting models for

these flow-sediment interactions, a predictor for the maximum saturation as developed here is essential. Moreover, it is expected that the degree of saturation differs between ideal situations of theoretical mixtures and real situations where a bed progressively fills.

The next section briefly describes the characteristics of packing porosity models and their utility for the study of natural sediments. Then the theoretical basis for the new method is presented and it is applied to experimental and field data found in published literature; this is followed by a discussion and conclusions.

## APPLICATION OF PACKING POROSITY MODELS TO NATURAL SAND–GRAVEL BEDS

Size gradation of bed material in gravel and sand–gravel bed rivers usually has two distinct modes: one for the size range of sand (<2 mm) and the other for the size range of gravel (>2 mm). Therefore, for practical purposes, the bed material can be considered a mixture of sand and gravel (e.g. Wilcock, 2001). According to the amount of sand in the mixture, the bed structure of a gravel deposit lies between two extreme regimes: (i) open-framework gravel, in which the bed is composed only of gravel; and (ii) a sand matrix, with a total absence of large clasts. Three intermediate states can be identified between these two extremes: partially filled gravel, filled gravel and gravel dispersed in a sand matrix (Church *et al.*, 1987; see Fig. 1). In partially filled and filled gravel, gravel supports the bed structure; while in gravel dispersed in a sand matrix the coarse grains are not necessarily in contact with one another. In terms of sediment percolation processes, sand infiltration can only occur in deposits with partially filled or open-framework gravel. In these two states, there are more likely to be pores that are large enough to be occupied by particles smaller than the grains forming the bed skeleton (Fig. 1). Conversely, filled gravel would indicate a limit of sediment deposit, when the bed cannot receive any more sand particles. In fact, infiltration of fines depending on flood history and local environment of deposition has been one of the main mechanisms invoked by researchers for the formation of matrix-filled gravel (e.g. Smith, 1974; Frostick *et al.*, 1984; Carling & Gleister, 1987).

The structure of alluvial beds has similarities to the packing of spherical and non-spherical particles, analysed by particle packing density models. A number of empirical and semi-empirical models have been published that determine the volume fraction of solids in granular materials (e.g. Westman, 1936; Yu & Standish, 1988, 1991; Finkers & Hoffmann, 1998; Liu & Ha, 2002). These models were

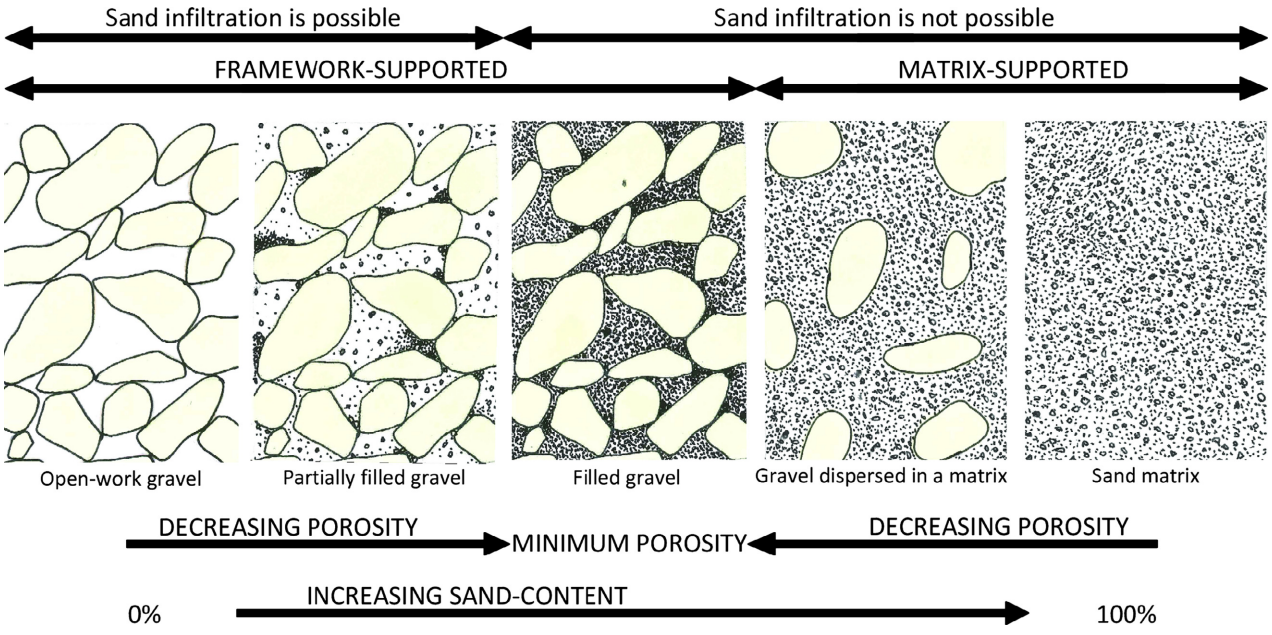


**Fig. 1.** Sketches of different conditions of bed structure as a function of relative sand content.

developed mostly for the chemical industry, where packing efficiency affects various processes, and maximization of the packing density of granular material products is a major factor in reducing transportation costs. Some applications of particle packing models to natural sediment (e.g. Koltermann & Gorelick, 1995; Frings *et al.*, 2008, 2011) have shown the potential to contribute to the understanding of sedimentary processes.

The most elementary porosity model for granular materials considers an idealized binary mixture, in which the size ratio, $r$, between fine and coarse particles, approaches zero. For a bed of unit volume, the total volume of solids would be $1 - \lambda$, where $\lambda$ is the bed porosity. If only the large particles support the bed structure, their total volume will be $1 - \lambda_D$, where $\lambda_D$ is their pure porosity. Accordingly, the relative proportion of coarse particles in relation to the total volume of solids can be written as $f_D = (1 - \lambda_D)/(1 - \lambda)$. If this relation is solved for the bed porosity, and stated as a function of the relative content of fine particles, which is equal to $f_d = 1 - f_D$, the following is obtained:

$$\lambda = \frac{\lambda_D - f_d}{1 - f_d} \qquad (1)$$

Equation 1 describes the change in bed porosity, as the fine size fraction subsequently infills the voids in the framework of large particles. When the fines have filled all the bed pores, i.e. when the bed is saturated, minimum porosity occurs. This porosity is equal to $\lambda_D\lambda_d$, that is, the product of the pure porosities, where $\lambda_d$ is the pure porosity of the fine particles. Equalling this product with Eq. 1, and operating, the result is:

$$\lambda = \frac{\lambda_d f_d}{1 - \lambda_d(1 - f_d)} \qquad (2)$$

Equation 2 shows the dependency of bed porosity on the characteristics of the fine size fraction, when this fraction forms a matrix in which the coarse particles are dispersed. Equations 1 and 2 define an idealized model for a densely packed mixture of two particle sizes. Both equations have been plotted in Fig. 2.

Empirical evidence has shown that the ideal model is never satisfied because the arrangement of each size fraction might be disturbed by the other component (McGeary, 1961), for instance, by small particles wedging in the framework of large grains (Dias *et al.*, 2004). It has been found that the interaction between size fractions depends on the size ratio. Different authors have proposed empirical relations to account for this effect, using experimental data based on obtaining random close packing. One of the most consistent empirical models found in the literature is that of Westman (1936) for spherical particles (see Appendix A). Finkers & Hoffmann (1998) modified the Westman model to extend its applicability to non-spherical grains (see Appendix A). The Westman model, as modified by Finkers & Hoffmann (1998), has been plotted in Fig. 2 for different values of the particle size ratio. The curves in Fig. 2 show that, as the values of $r$ increase, the porosity gradient with respect to the fines content, in the region of minimum porosity, becomes less steep. Dias

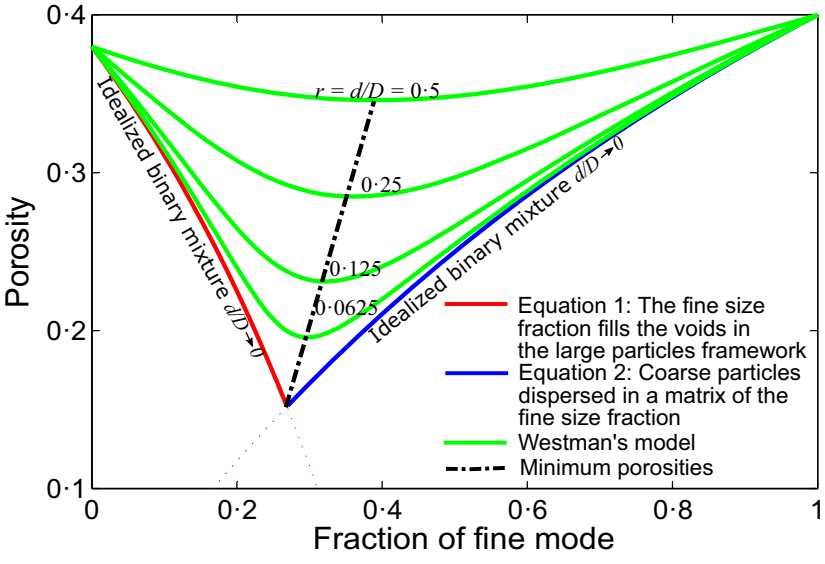


**Fig. 2.** Packing porosity models for binary mixtures. Idealized mixture (d≪D) and the Westman (1936) model for different particle size ratios according to the Finkers & Hoffmann (1998) correction for spherical and non-spherical particles with a narrow size distribution.

*et al.* (2004) related this behaviour to a more pronounced interaction between fractions when $0{\cdot}1 < r < 1{\cdot}0$. These authors suggested that for such moderate values of the particle size ratio, at the region around minimum porosity, the arrangement of small and large particles is unstable. Due to this instability, for this range of size ratios, the packing density is strongly dependent on the mixing procedure: if the mixture is obtained by filling a self-supporting skeleton of large grains with small particles (as occurs when the bed is filled by the infiltration of fines), a densely packed mixture may be obtained. Alternatively, if the mixing procedure is particle displacement and rotation (as occurs during simultaneous sedimentation of a heterogeneous mixture), the overall bed porosity may increase, because small grains can wedge between large ones.

## The Yu & Standish multifractional packing porosity model

Yu & Standish (1988, 1991) developed a multifractional porosity model, based on a detailed empirical description of the interaction between binary mixtures, which was then extended to arbitrary mixtures. The applicability of this model to any arbitrary number of size fractions makes it highly valuable to sedimentology, where extremely bimodal sediments are rare (Frings *et al.*, 2008). The method requires as input data a detailed grain-size distribution and an initial porosity, $\lambda_u$, for each size fraction, which refers to the porosity of a mixture of uniform sized grains.

In order to show the effect of non-uniformity of particles in porosity computations with the Yu & Standish (1991) model, in Fig. 3A the model results are presented for a combination of a uniform fine material with a coarse mixture (grain-size distributions shown in Fig. 3B), in the range of all possible relative proportions of the fine material. The same initial porosity, $\lambda_u$, has been considered for all grain-size fractions and materials, and five different standard deviations ($\sigma_c$) have been used for the mixture. The size ratio relating the mean diameters of the fine material and the mixture has been kept constant and equal to 0·2. For this same size ratio, the

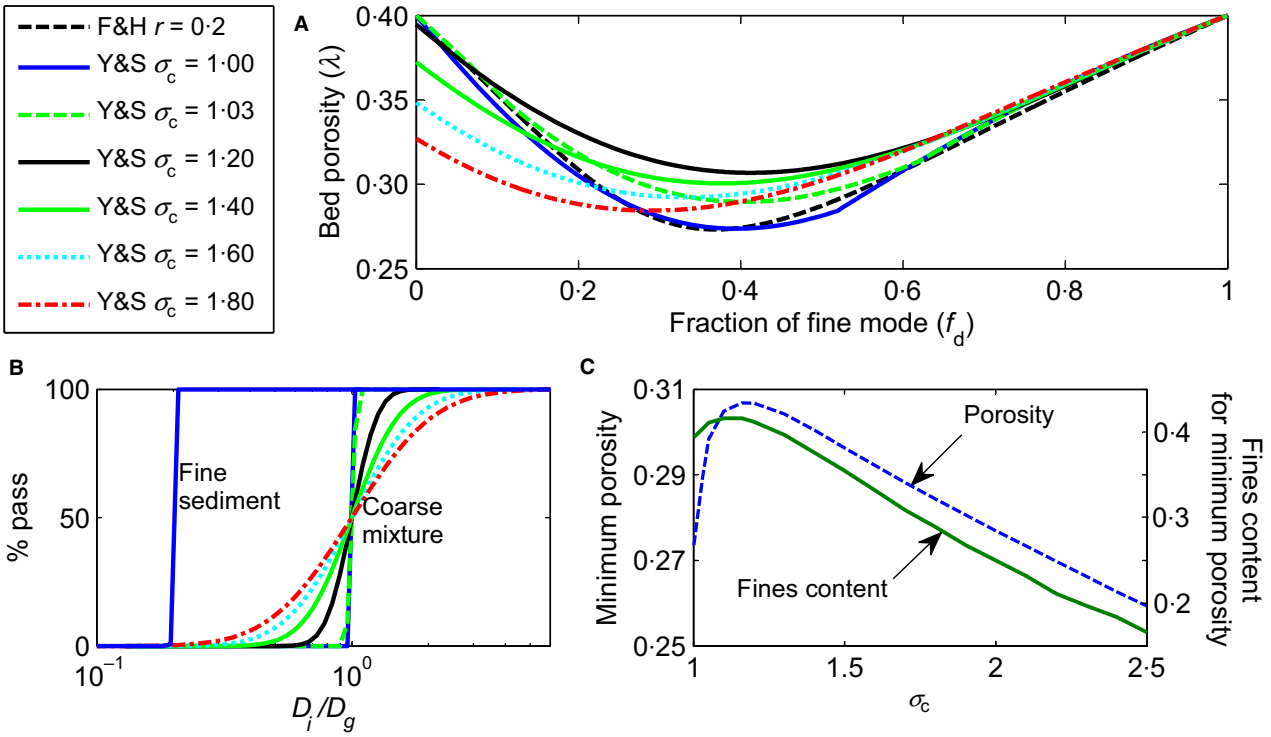


**Fig. 3.** (A) Computations with the packing porosity models of Finkers & Hoffmann (1998) (F&H) for binary mixtures and of Yu & Standish (1991) (Y&S) for multifractional mixtures for the combination of fine uniform material and coarse heterogeneous mixtures shown in (B). Different geometric standard deviations ($\sigma_c$) have been considered for the coarse mixture, but the size ratio between the mean diameters of the fine and coarse materials has been kept constant as equal to 0·2. The variation in minimum porosity and related fines content with $\sigma_c$ is shown in (C).

 

results of simulations with the Finkers & Hoffmann (1998) model for binary mixtures are also shown. In this example, for a uniform coarse material (mixture with $\sigma_c = 1$), the variation in porosity with the relative content of fines is almost identical for the two models, with a minimum porosity close to 0·28 occurring for a fines content value of almost 40%.

Figure 3C shows the variation in minimum porosity and the related fines content with $\sigma_c$, for the results with the Yu & Standish (1991) model. It is evident that the porosity increases for small increments in standard deviation in the coarse mixture, up to $\sigma_c = 1{\cdot}2$; however, for higher standard deviations there is an inverse proportionality between porosity and the mixture dispersion. This trend shows that, as long as the standard deviation of the mixture is low, all size fractions are subject to *occupation* effects, that is, they all form part of the bed skeleton (Yu & Standish, 1988). Conversely, for higher deviations, some small size fractions could fill the pores without disturbing the load-bearing larger particles. Consequently, the porosity is reduced by this *filling* effect (Yu & Standish, 1988). These interactions, which might be common in natural sediment mixtures, cannot be considered by the model for binary mixtures, because this model only takes into account the size ratio of the mean diameters to describe the mixture. Note that when the standard deviation of the mixture increases, the fractional content of fines for minimum porosity, computed with the multifractional model, shifts to lower values, with an approximate 20% difference between $\sigma_c = 1{\cdot}0$ and $\sigma_c = 2{\cdot}5$.

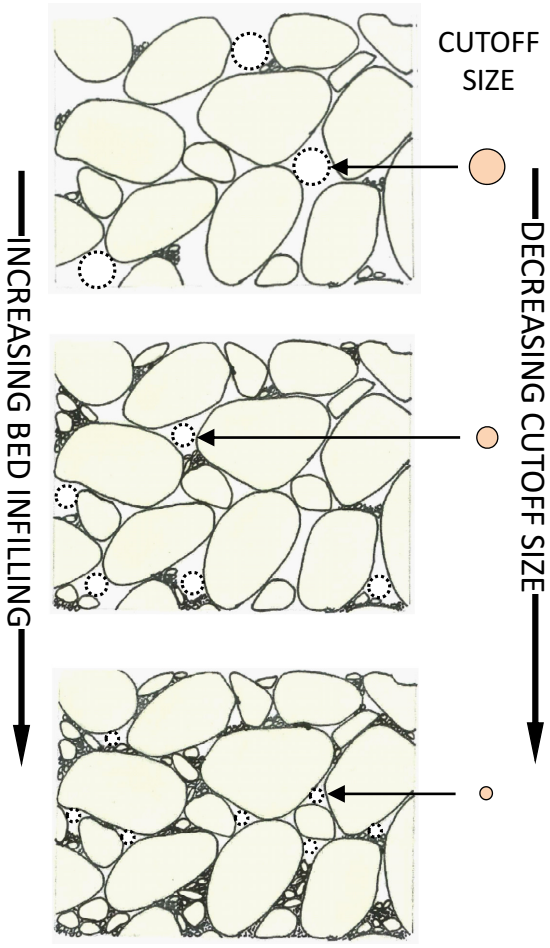


**Fig. 4.** Schematic representation of the change in bed cut-off size as the bed pores are filled with fines. The cut-off size indicates the limit for particle size classes that do not disturb the bed structure.

### *Computation of the bed cut-off size with the Yu & Standish model*

Frings *et al.* (2008) tested and adapted the Yu & Standish model for sediment applications. In particular, these authors used the model to predict the grain size in the boundary between particles that are still part of the bed structure, and particles that only fill the bed pores. With this cut-off grain size, Frings *et al.* (2008) distinguished the sediment that contributes to morphological changes in the bed ('pore-filling load') from the sediment that infiltrates through the pores in between the coarsest particles and does not interact with the bed structure ('bed-structure load'; see Fig. 4).

Frings *et al.* (2008) defined the cut-off size within the class limits of the diameter as equal to 0·154 times the central fraction of a bed 'controlling mixture', which is the mixture composed of the grain-size fractions that form the structure of the bed. The value of 0·154 is the maximum size ratio, $r_d$, between small and large spherical particles, that still allows small particles to fit into the pores of the larger particles, in the case of tetrahedral packing. Some authors consider that the value $r_d = 0{\cdot}154$ is also valid for natural grains with random tight packing (e.g. Soppe, 1990; McGeary, 1961; see review and procedure in Frings *et al.*, 2008).

Frings *et al.* (2008) found a slight underestimation of porosity for wide grain-size distributions, which was further confirmed in Frings *et al.* (2011), when the model was applied to four large data sets of laboratory and field porosity measurements in sediment mixtures. Despite these shortcomings, after a comparison of the performance of the model with another four porosity predictors, Frings *et al.* (2011)

showed that this model had the best theoretical basis and lowest prediction error.

## SUGGESTED METHOD TO ESTIMATE BED SATURATION

Filled gravel defines the state in which the void space within a self-supporting gravel framework is completely filled with sand (Fig. 1). Therefore, this condition defines the boundary between a gravel framework and gravel dispersed in a sand matrix, and the sand content in filled gravel indicates an inflection point of minimum bed porosity. Filled gravel could stand for the minimum porosity described in packing porosity models (see Fig. 2). If the infiltration of fine sediment in an immobile bed is conceived as successive infilling of framework gravel with sand, then the filled gravel condition would be equivalent to the stable saturated state. In this state, additional sand grains could only be admitted into the bed if the structure was altered.

Apart from filled gravel, a second limiting state can be defined for the infiltration of particles as the maximum packing density likely to be attained by a randomly poured sediment mixture. It may be hypothesized that bed packing generated through consecutive infiltration of fines might ultimately reach a dense packing state for which no more sediment intrusion is possible, when the bed porosity matches the porosity for 'random close packing' of the mixture.

Packing porosity models may prove useful for identifying the limiting packing condition. Experimental packings, used to develop the porosity models, are normally obtained by tapping and shaking a mixture of spheres to generate random close packing, so these models are a good indication of likely minimum porosities (Alberts, 2005). Random close packing results in a maximum density of *ca* 64% for hard uniform spheres, as reported by various authors (e.g. Scott & Kilgour, 1969). At the other extreme, the loosest random arrangement of a granular material, called 'random loose packing', is related to a value of maximum density of *ca* 55% for hard uniform spheres, according to different experimental results (e.g. Onoda & Liniger, 1990). Because a jam of randomly close-packed grains would not accommodate more particles of the same jammed species (no further loss of porosity would be possible) without altering the bed structure, random close packing would mark an extreme limit for percolation. Although the sort of arrangement found in random close packing is highly improbable, using a conservative estimate, it might be assumed that random close packing could be comparable to the stable saturated state of infiltrating fines. In developing a method to identify the conditions of saturated beds, it may thus be hypothesized that, during the infiltration of particles, the bed porosity is progressively reduced from an initial value between minimum random close packing and maximum random loose packing, to a minimum porosity, associated either with the complete infilling of the framework or a state resembling random close packing.

### Procedure to estimate bed saturation

To illustrate the new method of identifying the limiting packing density during fines infiltration, consider a bed composed of a binary mixture with particle size classes $D$ and $d$, where particles $d$ are much finer than particles $D$, and also much finer than the bed pore openings. Bed porosity $\lambda$ would be a function of the fractional content $f_d$ of $d$ particles, and of the packing arrangement of the particles. Packing models require as input the initial porosities for each of the species of particles. For simplicity, this initial porosity can be denoted again as $\lambda_u$, and can be considered as the same for the two size fractions, i.e. $\lambda_u = \lambda_D = \lambda_d$. It can be assumed that for any given value of $f_d$, there is a finite range of likely packing porosities, related to the arrangement of the particles in the bed, and that each value of $\lambda_u$ considered in a packing model would be related to only one of these packing compositions. In consequence, packing efficiency, i.e. packing density, would be directly proportional to $\lambda_u$, and manipulation of this input value can serve to simulate different packing arrangements. Represented accordingly as:

$$\lambda_j = \lambda_{PM}(\lambda_{u_j}, f_d) \quad (3)$$

where subscript $j$ denotes a given packing mode, $\lambda_{PM}$ indicates the algorithm followed by a given packing model to compute porosity, and $\lambda_u$ is the initial porosity. Equation 3 has been plotted with continuous lines in Fig. 5, for five different initial porosities $\lambda_u$, using the Finkers & Hoffmann (1998) model. For a given $\lambda_u$, related to a given packing mode $j$, $\lambda$ decreases as $f_d$ increases from zero up to a value where an inflection point of minimum porosity occurs.

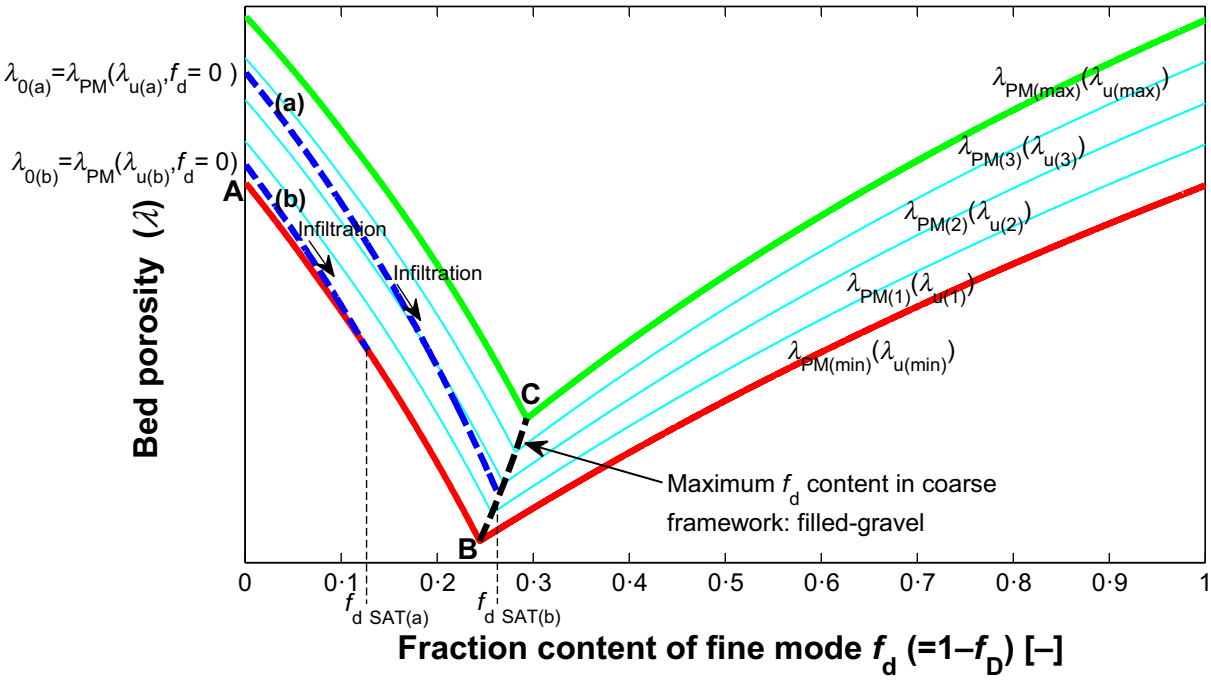


**Fig. 5.** Bed porosity variation in a binary mixture as a function of fractional content of fine mode $f_d$, for different packing arrangements: random close packing (red), random loose packing (green) and three intermediate packing arrangements (cyan). Variation in bed porosity due to infiltration of particles of fine mixture $f_d$ is shown as well (dashed-blue lines), for two initial bed porosities, 'a' and 'b'. The dark dashed line *BC* indicates the dominion for filled gravel.

This point of inflection would represent the filled gravel state, for the packing arrangement *j*. The range of minimum porosities for any number of *j* packing modes, in the domain of all possible $\lambda_u$ values within the selected extremes, is indicated by line *B–C* in the graphic. The $f_d$ values situated to the left of *B–C* would indicate a bed structure similar to a partially filled gravel framework, while those to the right correspond to gravel dispersed in a sand matrix.

To take into account the densest and loosest packing arrangements, the lowermost line in Fig. 5 (red continuous line) may be considered the porosity $\lambda_{RCP}$, related to a minimum random close packing state, and the uppermost line (the green continuous line) as the porosity $\lambda_{RLP}$, related to the maximum random loose packing, hence:

$$\lambda_{RCP} = \lambda_{PM}\left(\lambda_{u(min)}, f_d\right) \tag{4a}$$

$$\lambda_{RLP} = \lambda_{PM}\left(\lambda_{u(max)}, f_d\right) \tag{4b}$$

where $\lambda_{u(min)}$ and $\lambda_{u(max)}$ are the initial porosities, which can be taken as equal to the values associated with random close packing and random loose packing for uniform spheres, i.e. 0·36 and 0·45, respectively. The range of porosities in Eq. 4a, in the domain of $f_d$ from zero up to the inflection of minimum $\lambda_{RCP}$, indicate the limit for percolation related to random close packing. Similarly, the domain of $f_d$ in the range of minimum porosities in Eq. 3, from minimum $\lambda_{RCP}$ to maximum $\lambda_{RLP}$, indicates the limit for percolation related to filled gravel. In consequence, the limit for percolation (i.e. the condition for saturation) is defined by the curves *A–B* and *B–C* in Fig. 5.

If particles with size *d* progressively fill up the voids without changing the total volume in the bed, the volume of voids filled up would be controlled by the proportion of *d* grains in the bed mixture. Hence, the evolution of bed porosity as a function of the degree of filling can be described by Eq. 1, which outlines the decrease in bed porosity as the voids in a coarse framework are subsequently filled with fine grains. In Eq. 1, $\lambda_D$ would represent the initial bed porosity $\lambda_o$ at the beginning of infiltration, and $f_d$ the fractional content of *d* particles, so that Eq. 1 can be rewritten for the bed porosity $\lambda_{inf}$ during the infiltration process as:

$$\lambda_{inf} = \frac{\lambda_0 - f_d}{1 - f_d} \tag{5}$$

When Eq. 5 matches up with the curve for the random close packing or the filled gravel conditions, the limiting packing state would occur. Hence, the domain of Eq. 5 is the interval $0 \le f_d \le f_{dSAT}$, with $f_{dSAT}$ being the fractional content of $d$ size class in the saturated state.

Equation 5 has been plotted in Fig. 5 with blue dashed lines [labelled (a) and (b)], for two initial bed porosities ($\lambda_{0_{(a)}}$ and $\lambda_{0_{(b)}}$). The intersection of lines (a) and (b) with curves *A–B* and *B–C*, respectively, indicates the point of saturation due to random close packing limitations for the first line, and filled gravel restrictions for the second. For random close packing limitations, the equality $\lambda_{inf} = \lambda_{RCP}$ defines the intersection, in which $f_d = f_{d_{SAT(RCP)}}$, where $f_{d_{SAT(RCP)}}$ is the saturated value of $f_d$ for restrictions due to random close packing. Then, by matching Eqs 5 and 4a and solving them, an implicit relation for $f_{d_{SAT(RCP)}}$ is obtained as such:

$$f_{d_{SAT(RCP)}} = \frac{\lambda_0 - \lambda_{PM}\left(\lambda_{u(min)}, f_{d_{SAT(RCP)}}\right)}{\left(1 - \lambda_{PM}\left(\lambda_{u(min)}, f_{d_{SAT(RCP)}}\right)\right)} \tag{6}$$

Conversely, an implicit expression for the saturated value of $f_d$ due to filled gravel, $f_{d_{SAT(FG)}}$, can be obtained by equalling Eqs 5 and 3, i.e.:

$$\lambda_{PM}\left(\lambda_{u_j}, f_{d_{SAT(FG)}}\right) = \frac{\lambda_0 - f_{d_{SAT(FG)}}}{1 - f_{d_{SAT(FG)}}} \tag{7}$$

$f_{d_{SAT(FG)}}$ exists if there is a value $\lambda_{u_j}$ for which the first derivative of Eq. 3 evaluated at $f_{d_{SAT(RCP)}}$ is zero, that is $\lambda'_j = \lambda'_{PM}\left(\lambda_{u_j}, f_{d_{SAT(FG)}}\right) = 0$. Finally, the saturated fractional content of $d$ is obtained from the minimum value of $f_{d_{SAT(RCP)}}$ and $f_{d_{SAT(FG)}}$, that is $f_{d_{SAT}} = \min\left(f_{d_{SAT(RCP)}}, f_{d_{SAT(FG)}}\right)$.

Solutions of Eqs 6 and 7 using the Finkers & Hoffmann (1998) model for binary mixtures are shown in Fig. 6. The overall trend is a steep increase in the saturated content of fines for low initial bed porosities, or a shallower increase for higher initial bed porosities.

## Numerical implementation of the method for multifractional mixtures

The method described by Eqs 6 and 7 for estimating the fractional content of fines in the saturation state can be implemented to consider any arbitrary number of size fractions using a numerical computation. Finite increments in infilling fines may be aggregated over time, to test at each time step whether the computed porosity fulfils the conditions of saturation. A modified version of the theory for infiltration of fine sediment into an immobile bed, developed by Cui *et al.* (2008) for uniform infiltrating mate-

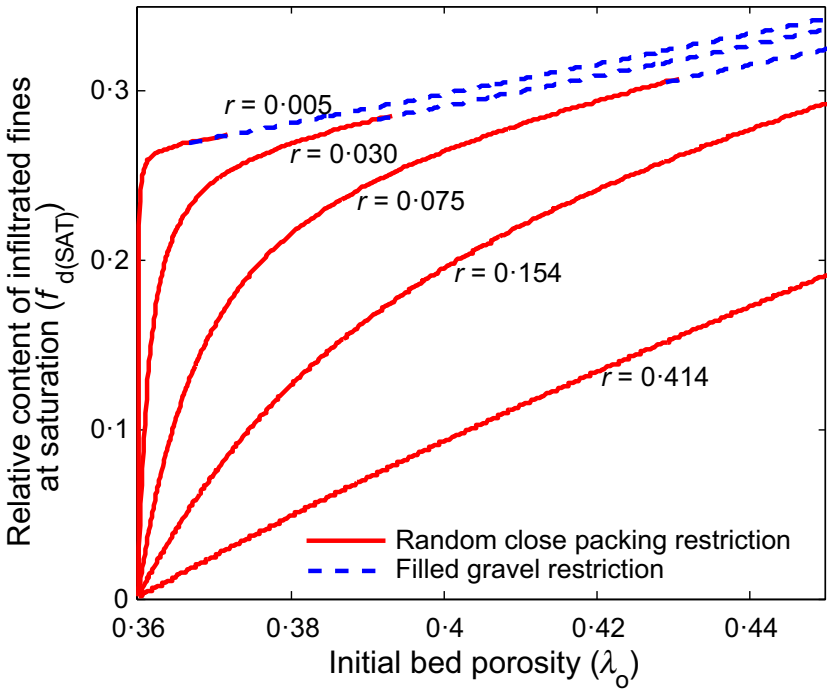


**Fig. 6.** Fractional content of infiltrated fines in the stable state as a function of considered initial bed porosity, obtained using the new method with the Finkers & Hoffmann (1998) model for binary mixtures. $r$ is the fine to coarse size ratio. Dashed lines indicate bed saturation due to filled gravel, while red lines indicate saturation due to minimum porosity related to random close packing.

rial, may be applied to formalize this procedure. In order to generalize this theory to consider heterogeneous mixtures, the continuity equation for a vertical flux of sediment, in a finite volume of unit bottom-surface area, is formulated for each size fraction $i$ as follows:

$$\frac{\partial C_i}{\partial t} + \frac{\partial q_i}{\partial z} = 0 \tag{8}$$

where $C_i$ is the total fraction of the finite volume occupied by sediment grains of size $i$, $q_i$ is the downward flux of particles of size $i$ per unit area entering into the finite volume, $t$ is time and $z$ is the vertical distance into the sediment deposit (in a downward direction). If all sediment entering in the finite volume is trapped within it, the integration of Eq. 8 along the vertical yields:

$$\frac{\partial C_i}{\partial t} = \frac{q_i}{\Delta z} \tag{9}$$

where $\Delta z$ is the thickness of the finite volume. Expressed in finite differences, Eq. 9 can be written as:

$$C_i|^{t+\Delta t} = C_i|^t + q_i|^t \frac{\Delta t}{\Delta z} \tag{10}$$

where $\Delta t$ is the time step. The incoming sediment in the finite volume is restricted by the size of the pore openings and the availability of void space; hence, by defining a constant total sediment incoming rate $q_T$ at any time $t > 0$, the incoming sediment flux into the finite volume for size fraction $i$ can be written as:

$$q_i(0, t>0) = \begin{cases} f_i q_T & \\ 0 & \text{if } \frac{d_i|^t}{D_c|^{t-\Delta t}} \geq 1 \\ 0 & \text{if } \frac{C_i}{C_{SATi}}|^{t-\Delta t} = 1 \end{cases} \tag{11}$$

where $C_{SATi}$ is the total fraction of the finite volume occupied by grain-size class $i$ when the bed is saturated, $D_c$ is the grain-size limit for particles that can fit into the bed pores, $d_i$ is the grain-size class $i$ of the infiltrating sediment, and $f_i$ is the fractional content of size $i$ in $q_T$, which is the total sediment downward flux. Then, $q_T = \sum_{i=1}^{n} q_i$, where $n$ denotes the total number of size classes in the bed and in the material penetrating the finite volume, ordered from coarse ($i = 1$) to fine ($i = n$). A stable condition for Eq. 10 is reached when $q_i = 0$ for all size fractions. Finally, for the equations above, at any time step, Eq. 12 can be used to transform the sediment gradation from fractional content by volume to fractional content by weight:

$$F_i = \frac{C_i}{\sum_{i=1}^{n} C_i} \tag{12}$$

where $F_i$ is the fractional content by weight of size fraction $i$ in the finite volume, and $C_i$ is related to the bed porosity by:

$$\sum_{i=1}^{n} C_i = 1 - \lambda \tag{13}$$

The bed cut-off size defined by Frings *et al.* (2008), to be computed with the Yu & Standish model, fits the requirements to stand in for $D_c$ in Eq. 11. As shown before, the Frings *et al.* (2008) cut-off size serves as an indicator of the size fractions that can percolate because they do not disturb the bed structure (see Fig. 4). Therefore, this method can be used within the algorithm to identify the saturated conditions of a bed progressively filled with infiltrating sediment. According to the data required to compute the bed cut-off size with the Yu & Standish model, it can be stated for $D_c$ at each time step:

$$D_c|^t = D_{c_{FYS}}\left[(D_1,\ldots,D_{i=n};F_1,\ldots,F_{i=n})^t, r_d, \lambda_u\right] \tag{14}$$

where $D_{c_{FYS}}$ indicates the functional relation solved by the algorithm to compute the cut-off size with the procedure developed by Frings *et al.* (2008) using the Yu & Standish method, $F_i$ is defined by Eq. 12, $r_d$ is the critical size ratio for the infiltration of particles, and $\lambda_u$ is the pure porosity of each size fraction. For accurate predictions of the cut-off size, a sensitivity analysis performed by Frings *et al.* (2008) showed that at least eight size classes should be used to define the 'body' of the grain-size distribution, and that the size class width should be, at most, 0·5 phi in the fine tail of the distribution. In addition, Frings *et al.* (2008) suggested that the cut-off size is independent of $\lambda_u$, as long as this porosity ranges from 0·3 to 0·5. Due to discretization of the grain-size distribution, the Yu & Standish method defines the cut-off size at one class limit between grain-size fractions. For comparison with this value in Eq. 11, $d_i$ is here defined as the centre of class of the infiltrating sediment, such that $d_i = (d_N d_{N+1})^{0.5}$, where $N$ denotes the $N$th size class limit. Although Yu & Standish (1991) used a value of $r_d$ related to

tetrahedral packing, there is no clear evidence of the most suitable value in natural sediments.

In order to assess whether the bed has attained saturation during simulations, bed porosity must be known at every time step. For the initial conditions, it is assumed that the bed grain-size distribution is known. Thus, the initial bed porosity $\lambda|^{t=0}$ can be obtained from the Yu & Standish method. The calculated initial porosity can then be used to compute the initial fractional content by volume of each grain-size fraction as $C_i = F_i(1 - \lambda)$. For subsequent time steps, bed porosity is calculated by solving Eq. 13, and $F_i$ is obtained using Eq. 12. Finally, it can be stated that the bed is saturated with infiltrating sediment, if the finest supplied size fraction is larger than the bed cut-off size, or if the bed porosity fulfils one of the following conditions at any given time step:

$$\text{if } \lambda|^{t} \begin{cases} = \lambda_{YS}\left[(D_1,\ldots,D_n;F_1,\ldots,F_n)^{t}, r_d, \lambda_{u(\min)}\right], C_{SATi} = C_i|^{t} \\ \geq \lambda_{YS}\left[(D_1,\ldots,D_n;F_1,\ldots,F_n)^{t-\Delta t}, r_d, \lambda_{u_j}\right], C_{SATi} = C_i|^{t-\Delta t} \end{cases} \quad (15)$$

where $\lambda_{YS}$ indicates the functional relation solved by the algorithm to compute packing porosity with the Yu & Standish model, $\lambda_{u(min)} = 0{\cdot}36$, in agreement with the minimum random close packing of spherical particles, and $\lambda_{u_j}$ might be calculated by an iterative process, so that it satisfies $\lambda|^{t} = \lambda_{YS}[\lambda_{u_j}, (D_1,\ldots,D_n;F_1,\ldots,F_n)^{t}]$. The first condition in Eq. 15 takes into account random close packing limitations, while the second condition represents filled gravel restraints. When any of these conditions is met, or when the cut-off size is smaller than any of the size fractions prone to infiltrate, the stable state is attained and the overall computation of sediment infiltration stops.

## APPLICATION TO EXPERIMENTAL DATA IN LITERATURE

### Selected data and general assumptions for application of the method

The suggested method for estimating the bed grain-size distribution on the saturation state is tested here with published experimental data. Selected data sets are summarized in Table 1. For all of the selected experiments, water and fine sediment were constantly fed into a flume with a bed composed of gravel, which for most of the runs remained immobile. The experiments were finished when no more infiltration of fine particles was observed, that is, when the saturation state was attained on the surface layer. The authors obtained samples of the bed material at different depths. From these samples, for testing the new method the characteristics of the surface layer were used, in which it is very likely that saturation might have been attained. The measured average final content of infiltrated fines for this layer is indicated in the last column of Table 1.

For a bed progressively filled with heterogeneous fine particles, the final saturation state is dependent on the initial bed porosity, as well as on the bed and the grain-size distribution of the infiltrating fines, as defined by Eqs 10 to 15. These equations were applied using as input values the initial grain-size distribution of the experimental gravel beds, the grain-size distribution of the feeding fines, and a range of likely initial porosities $\lambda_u$ for each size fraction. The depth increments chosen for the simulations were equal to 0·01 m, which was the thickness of layers in the bed core samples in most of the experiments summarized in Table 1. This value is also close to the mean diameter of the bed sediment in the selected experiments, and is the value used by Viparelli *et al.* (2010) and Ferrer-Boix & Hassan (2014) for morphodynamic simulations with changing vertical stratigraphy.

Before the method was applied to all of the experiments summarized in Table 1, a series of simulations were performed using data items 1 to 16, to assess the sensitivity of the results to the selected time and depth increments. For this purpose, a dimensionless parameter $\alpha$ was defined, as the ratio between the mass volume entering into the bed at each time step, and the volume-space in the defined finite volume of unit bottom area, i.e. $\alpha = q_T\Delta t/\Delta z$. Tested values of $\alpha$ ranged from $5 \times 10^{-6}$ to $5 \times 10^{-2}$, while five initial porosities $\lambda_u$, and two grain-size ratios ($r_d = 0{\cdot}154$, tetrahedral packing; $r_d = 0{\cdot}414$, cubic packing) were used in the Yu & Standish (1991) model. It was found that for approximate values of $\alpha < 1 \times 10^{-4}$, $\alpha$ had a negligible effect on the predicted infiltrated

**Table 1.** Selected experimental data

| ID | Data set | Run number (Z = zone, S = fed material) | Bed sediment characteristics | | Feed material | | Average saturated fines content $F_{f,SAT}$ |
|---|---|---|---|---|---|---|---|
| | | | $D_m$ [mm] | $\sigma_g$ | $d_m$ [mm] | $\sigma_g$ | |
| (1) | Beschta & Jackson (1979) | 1 to 18, 21 (S1) | 13·5 | 1·57 | 0·50 | 1·55 | 2 to 8% ≈5%* |
| (2) | | 19 and 20 (S2) | | | 0·20 | 1·61 | 25%* |
| (3) | Wooster *et al.* (2008) | 1 (Z1) | 7·2 | 1·87 | 0·35† | 1·24 | 6%‡ |
| (4) | | 1 (Z2) | 10·2 | 1·77 | | | 11%‡ |
| (5) | | 1 (Z3) | 13·1 | 1·68 | | | 12%‡ |
| (6) | | 1 (Z4) | 17·2 | 1·17 | | | 17%‡ |
| (7) | | 1 (Z5) | 7·4 | 1·90 | | | 5%‡ |
| (8) | | 1 (Z6) | 7·9 | 1·22 | | | 12%‡ |
| (9) | | 1 (Z7) | 8·7 | 1·71 | | | 7%‡ |
| (10) | | 1 (Z8) | 7·6 | 1·46 | | | 5%‡ |
| (11) | | 1 (Z9) | 4·3 | 1·65 | | | 5%‡ |
| (12) | | 1 (Z10) | 7·2 | 1·87 | | | 6%‡ |
| (13) | Gibson *et al.* (2009) | 1 (S-IFS1) | 7·1 | 1·37 | 0·43 | 1·70 | 25%§ |
| (14) | | 2 (S-IFS2) | | | 0·26 | 1·94 | 20%§ |
| (15) | | 3 (S-IFS3) | | | 0·21 | 1·55 | 20%§ |
| (16) | | 4 (S-IFS4) | | | 0·12 | 1·37 | – |
| (17) | Gibson *et al.* (2010) | 8 (Z1-Sand 6) | 9·7 | 1·27 | 0·21 | 1·55 | 25%§ |
| (18) | | 8 (Z2-Sand 6) | 7·2 | 1·39 | | | 20%§ |
| (19) | | 8 (Z3-Sand 6) | 6·0 | 1·19 | | | 20%§ |
| (20) | | 8 (Z4-Sand 6) | 5·3 | 1·24 | | | 14%§ |
| (21) | | 8 (Z6-Sand 6) | 3·7 | 1·25 | | | 21%§ |
| (22) | | 8 (Z8-Sand 6) | 2·9 | 1·10 | | | 22%§ |
| (23) | Gibson *et al.* (2011) | 1 (S1) | 7·7 | 1·41 | 0·65 | 1·58 | 20%§ |
| (24) | | 2 (S2) | 7·7 | 1·41 | 0·36 | 1·66 | 19%§ |
| (25) | | 3 (S2) | 9·7 | 1·27 | 0·36 | 1·66 | 31%§ |

*Fractional content by volume. †Grain-size distribution for this material was not reported. It is here considered that it was log-normally distributed. ‡The saturated layer occurred under a coarse armour layer. Approximate average values obtained from data in fig. 7 in Wooster *et al.* (2008). §Approximate values obtained from the surficial layer in figures presented by the authors, with the average vertical distribution of fines.

fines. For all of the computations presented in this work, $q_T$ and Δt were chosen so that the resulting α was always lower than $1 \times 10^{-3}$.

## Results of simulations

### *Fines content as a function of initial bed porosity*

For eight of the data items in Table 1, the saturated states resulting from the simulations are shown as a function of initial bed porosities in Fig. 7, for size ratios related to tetrahedral and cubic packing. The results for the rest of the data showed similar trends. The range of initial bed porosities, for each curve in Fig. 7, corresponds to porosity computations with the Yu & Standish model, using porosities of uniform material $\lambda_u$ ranging from the minimum random close packing and the maximum random loose packing of hard uniform spheres. To estimate the cut-off size at each time step using Eq. 14, the value for the minimum random close packing of hard uniform spheres was used for $\lambda_u$.

Similarly, as in computations with the model for binary mixtures shown in Fig. 6, the increments in final infiltrated fines content with respect to initial bed porosities ($\lambda|^{t=0}$) in Fig. 7 were steep for low initial porosities on each curve. The increments were steeper for most of the data when $r_d = 0{\cdot}414$ rather than $r_d = 0{\cdot}154$. This steep gradient of final fines content would be related to the saturation ascribed to the minimal porosity of the mixture due to a maximum packing density limitation (random close packing restriction), i.e. the limit set by line *A–B* in Fig. 5.

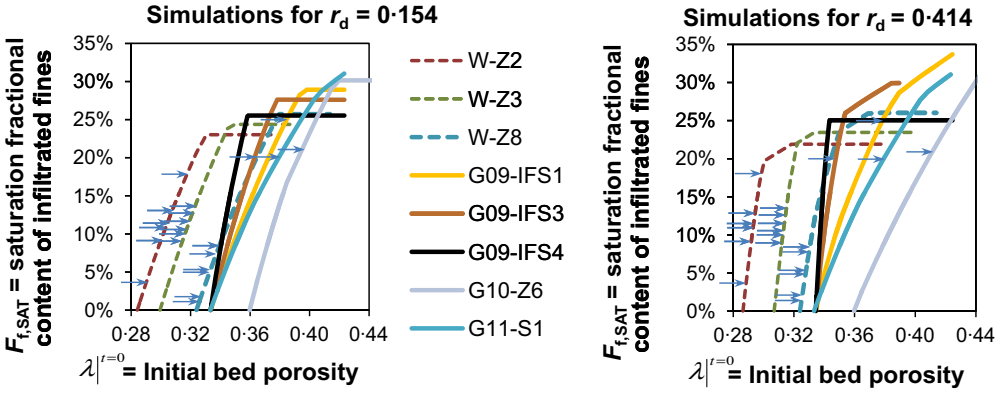


**Fig. 7.** Simulated fractional content of infiltrated fines in the stable state, as a function of estimated initial bed porosity. $r_d$ is the maximum fine to coarse size ratio allowing infiltration, used in the Yu & Standish (1991) model. Simulations were performed using grain-size distributions of eight of the experimental data in Table 1. Experimentally measured fines content for the saturated layer from individual samples (if available) are shown with arrows. W = Wooster *et al.* (2008); G09 = Gibson *et al.* (2009); G10 = Gibson *et al.* (2010); G11 = Gibson *et al.* (2011).

For most of the curves in Fig. 7, there is a limiting value of porosity above which there is no increment in infiltrated fines with porosity (i.e. the saturated fines fraction is not dependent on the initial bed porosity). This trend contrasts with that shown in Fig. 6 for the binary mixtures model, where the fines content associated with saturation increases throughout the range of initial porosities. The plateau in the curves of Fig. 7, for high initial porosities, would be explained by saturation related to a cut-off size that is smaller than any of the size fractions supplied. Because the bed is filled with fines in simulations, and the bed grain-size distribution becomes finer, the computed cut-off size decreases (see Fig. 4). For high initial porosities, the bed can receive a large amount of fines, so that before it reaches the limiting porosity related to random close packing, there is a moment when the amount of fines in the bed is so high that the cut-off size becomes smaller than the size of the smallest supplied particles. Therefore, insensitivity of the final fractional content of fines to the initial porosity evidenced in Fig. 7 would be related to a lack of sediment supplied from above that is finer than the pore openings. Such an effect cannot be captured by computations using the model for binary mixtures, since that model does not consider a reduction in pore opening size with infiltration.

### *Back-calculated initial bed porosities*

For all of the experimental data in Table 1, the researchers confirmed that when a run was stopped there were no more particles penetrating the bed. Hence, it can be assumed that the final conditions were equivalent to the stable state, and that either the surface layer was saturated or its cut-off size was smaller than the finest grain-size fractions in contact with the bed surface. These final conditions can serve to estimate the initial porosities of the experimental beds using the new method. The initial porosities $\lambda_u$ and $\lambda|^{t=0}$ which resulted in final infiltrated fines in the surface layer equal to the average measured values, were obtained with simulations performed using a trial and error approach. These porosities are shown in Table 2 for the size ratio $r_d$ = 0·154. Results obtained using $r_d$ = 0·414 (not shown) were on average 2% lower than those using $r_d$ = 0·154.

The results of back-calculated initial porosities cannot be compared with experimental data, because the initial bed porosities were not given in any of the selected data sets in the experiments reported by the authors. Gibson *et al.* (2010) presented porosity values for loose and dense packing of the gravels used for experiments (data items 17 to 22 in Table 1), but did not indicate whether the initial state of the bed pertained to loose or dense packing. The porosities reported by Gibson *et al.* (2010) are compared in Fig. 8 with the initial bed porosities obtained with the simulations. The porosities from the simulations are on average 11% lower than the corresponding loose packing porosities, and 1% lower than the corresponding dense packing values. This outcome confirms that porosities computed with the Yu & Standish model tend to be underestimated, as reported by

**Table 2.** Results of applying the porosity model to the experimental data, considering tetrahedral packing: $r_d = 0{\cdot}154$

| ID | Data set | Zone or fed material | Computed initial bed porosities | | Stability constraint |
|---|---|---|---|---|---|
| | | | $\lambda_u\|^{t=0}$ | $\lambda\|^{t=0}$ | |
| (1) | Beschta & Jackson (1979) | (S1) | 0·370 | 0·314 | RCP |
| (2) | | (S2) | 0·384 | 0·328 | $d_n \geq D_c$ |
| | | | Mean = 0·321 ± 0·0069 | | |
| (3) | Wooster *et al.* (2008) | (Z1) | 0·372 | 0·288 | RCP |
| (4) | | (Z2) | 0·380 | 0·304 | RCP |
| (5) | | (Z3) | 0·381 | 0·320 | RCP |
| (6) | | (Z4) | 0·384 | 0·381 | RCP |
| (7) | | (Z5) | 0·369 | 0·280 | RCP |
| (8) | | (Z6) | 0·378 | 0·371 | RCP |
| (9) | | (Z7) | 0·372 | 0·303 | RCP |
| (10) | | (Z8) | 0·369 | 0·333 | RCP |
| (11) | | (Z9) | 0·370 | 0·315 | RCP |
| (12) | | (Z10) | 0·372 | 0·288 | RCP |
| | | | Mean = 0·318 ± 0·0327 | | |
| (13) | Gibson *et al.* (2009) | (S-IFS1) | 0·412 | 0·385 | RCP |
| (14) | | (S-IFS2) | 0·390 | 0·363 | RCP |
| (15) | | (S-IFS3) | 0·390 | 0·363 | RCP |
| (16) | | (S-IFS4) | – | – | $d_n \geq D_c$* |
| | | | Mean = 0·370 ± 0·0105 | | |
| (17) | Gibson *et al.* (2010) | (Z1) | 0·393 | 0·381 | RCP |
| (18) | | (Z2) | 0·393 | 0·367 | RCP |
| (19) | | (Z3) | 0·393 | 0·388 | RCP |
| (20) | | (Z4) | 0·384 | 0·375 | RCP |
| (21) | | (Z6) | 0·400 | 0·391 | RCP |
| (22) | | (Z8) | 0·398 | 0·397 | RCP |
| | | | Mean = 0·383 ± 0·0102 | | |
| (23) | Gibson *et al.* (2011) | (S1) | 0·401 | 0·373 | RCP |
| (24) | | (S2) | 0·392 | 0·364 | RCP |
| (25) | | (S2) | 0·409 | 0·396 | $d_n \geq D_c$ |
| | | | Mean = 0·378 ± 0·0138 | | |

*Because no information about the saturated fines content was provided, the initial bed porosity used for computations was the average from data 13, 14 and 15, which used the same gravel. RCP = Random close packing, stable state related to minimum porosity.

Frings *et al.* (2011). Even if the absolute values of computed initial porosities might not be completely accurate, their dispersion is in the range of realistic variations due to different degrees of settlement. As such, these results indicate that the new method performs well. New simulations were performed using the back-calculated porosities as initial conditions. For some of these simulations, the variation in bed porosity with time is shown in Fig. 9A.

For a clearer illustration of the likely effect of initial bed porosity on the final saturation state in simulations, the measured fines content of individual samples from the subsurface layer (presumably saturated) of three of the zones in the Wooster *et al.* (2008) experiments are shown with arrows in Fig. 7. The average final fines content shown in the last column of Table 1 is the average of all these samples. The coefficient of variation in computed initial porosities with each of these individual measurements was lower than 3% for the three zones, while this same parameter for the measured saturation fines content was as high as 62% for zone 8.

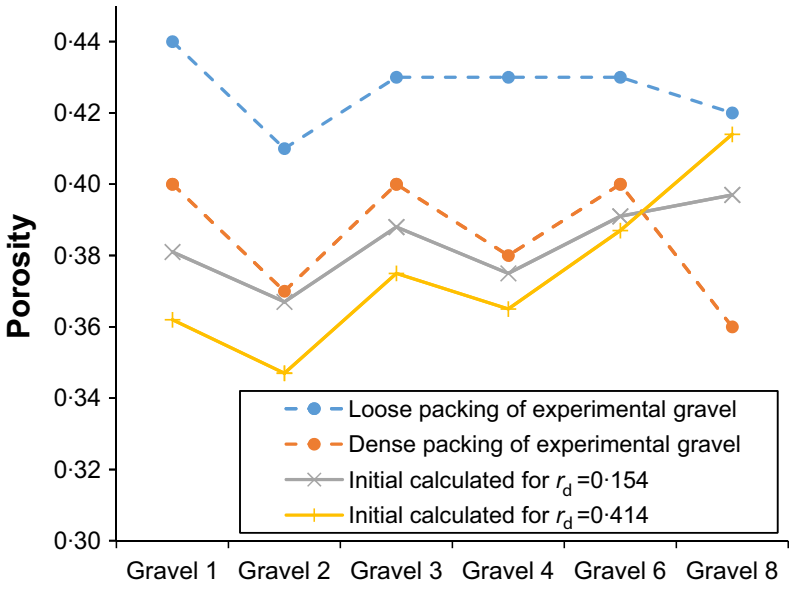


**Fig. 8.** Comparison of back-calculated porosities with simulations for the bed clean of fines, and porosity of the experimental gravels with loose and dense packing, for data from Gibson *et al.* (2010).

Wooster *et al.* (2008) found a large scatter when attempting to correlate the saturated fine fraction with statistical parameters of the coarse and fine sediment grain-size distributions. Given the results from the simulations presented here, this dispersion might be explained by large incre-

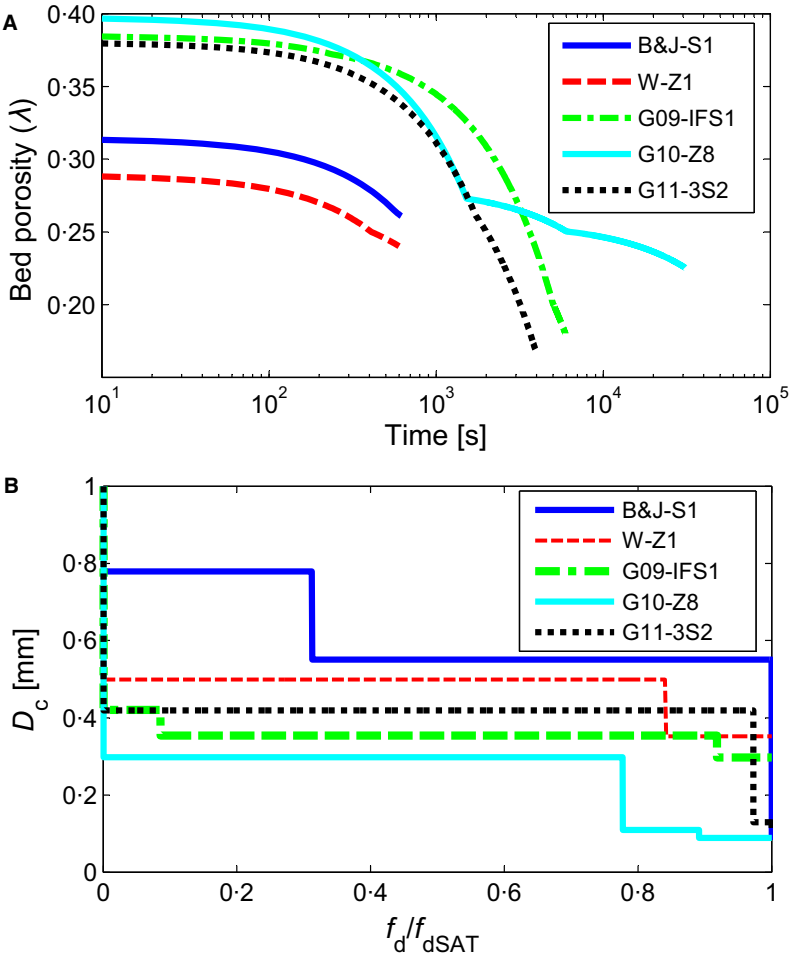


**Fig. 9.** Results for some of the simulations with published experimental data, using $r_d$ = 0·154, $q_T$ = 0·001 $m^3/s/m^2$, and back-calculated porosities as initial conditions. (A) Loss of bed porosity with time. (B) Variation in the computed cut-off size with the degree of infilling. B&J = Beschta & Jackson (1979); W = Wooster *et al.* (2008); G09 = Gibson *et al.* (2009); G10 = Gibson *et al.* (2010); G11 = Gibson *et al.* (2011).

ments in the final fines content related to slight variations in the initial bed porosity within zones of homogeneous bed material.

*Simulated bed cut-off sizes*

A comparison of computed cut-off sizes and the size gradation of experimentally infiltrated fines might serve as an assessment of the accuracy of the Yu & Standish model. For this comparison, data sets from Beschta & Jackson (1979), Wooster *et al.* (2008) and Gibson *et al.* (2009) are used, because these are the only authors that provided some information about the grain-size gradation of the experimentally infiltrated fines. For the same simulations previously described, for which the measured and simulated final fines content were forced to be the same, computed cut-off sizes for some of the experimental data, are shown in Fig. 9B as a function of the degree of saturation in simulations.

As illustrated in Fig. 4, during the infilling process the cut-off size can be expected to decrease as the fines content in the bed increases. This effect was reproduced by most of the simulations. Nevertheless, as shown in Fig. 9B, the cut-off size only changed once for most of the data and, in most cases, such changes were not significant in comparison to the grain size of the sediment supplied. This means that the supplied sediment was much finer than the immobile bed material, so that even for conditions when there were large amounts of infiltrated material in the bed, some pores were big enough to be filled by the fines. In this case, the most common constraint that limited further infiltration and promoted stability in the computations was the attainment of maximum packing density, i.e. a random close packing limitation, rather than a limitation in cut-off size. Consequently, changes in the grain-size distribution of the material that actually penetrated the bed would not have been relevant.

Wooster *et al.* (2008) observed that for all experimental conditions there was no selective infiltration of the feeding size fractions, so that the intruding and feeding materials must have had the same size gradation. Simulations reproduced this outcome, because the cut-off size was mostly larger than the maximum grain size in the feeding material, irrespective of tetrahedral or cubic packing.

Gibson *et al.* (2009) identified some grain-size segregation processes related to the flow and sediment transport interactions during experiments. In order to study infiltration without the effect of such processes, these authors performed additional experiments without flowing water, in which the fine sediment was poured from above. The results from these experiments showed that the median diameter of the poured fine material was approximately the same as that of the intruded sediment at saturation, except for their material IFS2, for which it was coarser. The experiments without flowing water from Gibson *et al.* (2009) would be better suited to compare the cut-off sizes obtained in the simulations, because the method here does not consider grain-size segregation due to flow and transport. In simulations that consider cubic packing, the computed cut-off sizes for the data of Gibson *et al.* (2009) were always larger than all grain-size fractions in the feeding material. Thus, such simulations reproduced the experimental outcomes correctly, except for material IFS2. Conversely, for tetrahedral packing, the computed cut-off size was smaller than the maximum feeding grain size, for three of the four runs; this resulted in the simulated infiltrated material being finer than the material fed. Hence, it can be concluded that for the Gibson *et al.* (2009) data set, simulations that considered cubic packing performed better than those that considered tetrahedral packing.

Out of all the selected experiments, the detailed grain-size distribution of the infiltrated sediment was only provided in data from Beschta & Jackson (1979), which used feeding fines of 0·5 mm mean diameter. This distribution is compared in Fig. 10 with the size gradation of the infiltrated material obtained from the simulations. For cubic packing, the estimated cut-off size was over four times greater than the $d_{95}$ of the feeding material. Therefore, the simulations resulted in the same grain-size distribution of intruded and feeding fines. Conversely, for tetrahedral packing, the computed bed cut-off size was 80% finer than the $d_{95}$ of the feeding material. Consequently, the infiltrated material in simulations was finer than the feeding sediment. This resulted in simulated and measured infiltrated fines sharing the same mode of 0·33 mm. It can thus be stated that, for this data set, the simulation results compare better to the experimental measurements using the size ratio for tetrahedral rather than cubic packing.

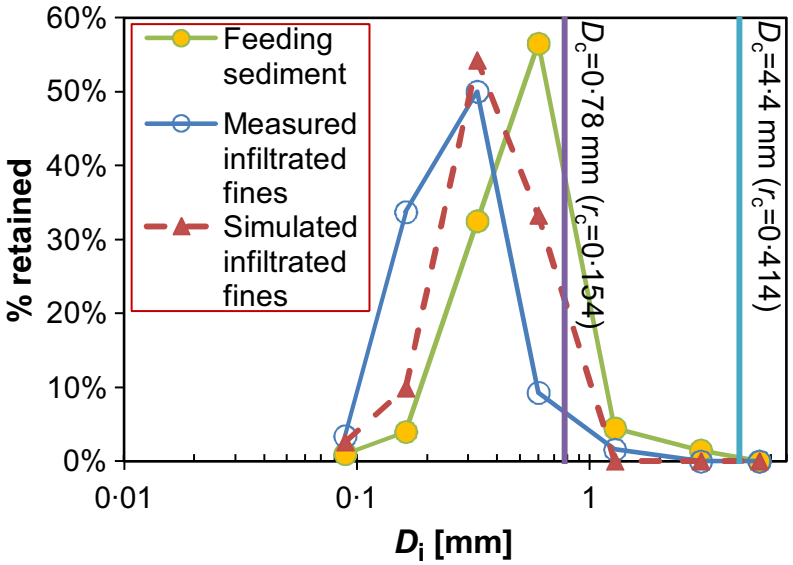


**Fig. 10.** Simulated and measured grain-size frequency distributions by weight of infiltrated fines, and feeding bed material, for experimental data from Beschta & Jackson (1979) using their coarsest sand. Simulations with a size ratio $r_d$ = 0·414 produced roughly the same distribution (data not shown) as the feeding material. Results with simulations using $r_d$ = 0·154 share the same grain-size mode with measurements.

## EXAMPLE OF APPLICATION TO FIELD DATA

To exemplify a likely practical use of the approach developed here, simulations were performed using data collected by Evans & Wilcox (2014) on a complex reach of a wandering gravel bed river. These authors aimed to identify spatial trends in bed siltation related to sediment supply and local flow dynamics. For this purpose, a number of sediment samples were obtained at different depths in four channel regions with distinctive hydraulic and depositional settings. Simulations with the new method were performed for samples of three of the regions investigated by Evans & Wilcox (2014) identified, respectively, as the riffles zone, shear zone and recirculation zones. Three of the samples presented by Evans & Wilcox (2014) from each region were used for the simulations, corresponding to the coarsest, the finest and an intermediate grain-size distribution. For each sample, a series of simulations was performed using initial uniform porosities $\lambda_u$ ranging from the minimum random close packing and the maximum random loose packing of hard uniform spheres, i.e. from 0·36 to 0·45. Infiltrating material was considered with the same grain-size distribution as the original bed material, but truncated at the bed cut-off size. In this manner, it was assumed that the fines supplied to each depositional setting contained the same fine size classes and relative proportions as in the corresponding bed material. Figure 11 shows the original grain-size distributions for the bed samples used to apply the model, and the saturated states obtained from simulations with $\lambda_u$ = 0·38 and $\lambda_u$ = 0·45. The riffles zone has been omitted from Fig. 11, because the grain-size distributions were quite similar to those obtained for the recirculation zone.

In all three regions, the difference between the original and simulated saturated grain-size distributions decreased with the amount of initial fines content. The sample with the highest initial sand content in Fig. 11, that is the fine sample in the recirculation zone, was the most extreme case, because the original and saturated grain-size distributions were almost identical. It is thus likely that the location corresponding to this sample was near saturation, and there would have been very limited pore space available for further fines infilling. A similar conclusion can be drawn for the fine sample of the shear zone. For the rest of the distributions, the saturation fines content increased with the initial uniform porosity used, but for the recirculation zone there was no significant difference if the initial uniform porosity considered was equal to or greater than 0·38.

Initial and final bed porosities obtained with the model, averaged over the whole range of studied porosities $\lambda_u$, and over the three samples in each region, are shown in Table 3. Average values of initial fractional contents of fines are also shown in this table. As expected, a negative trend between simulated porosities and the initial fractional content of fines is evident. For a quantitative description of the likely degree of saturation, a value of relative saturation can be

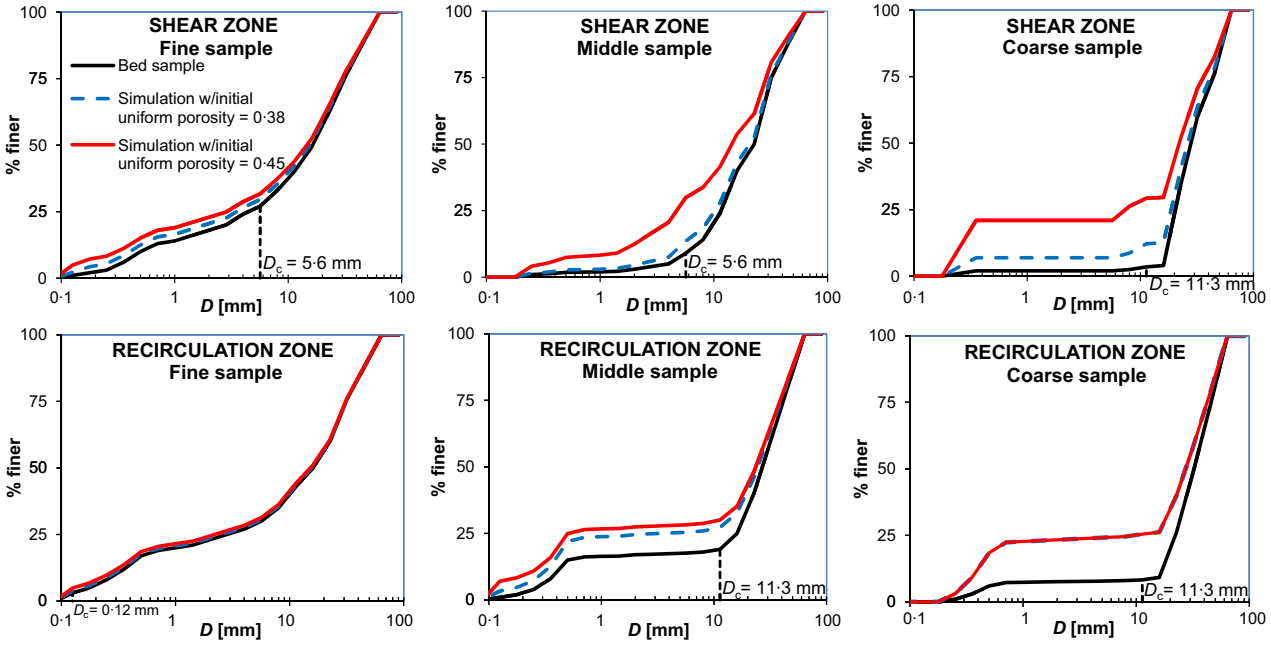


**Fig. 11.** Grain-size distributions for original bed samples presented by Evans & Wilcox (2014) and for saturation conditions resulting from simulations with two different initial porosities $\lambda_u$ for uniform material. Cut-off sizes $D_c$ indicated on each graphic correspond to the estimated values in the initial condition.

defined with respect to a reference porosity $\lambda_R$, as $(\lambda_R - \lambda_o)/(\lambda_R - \lambda_{inf})$, where $\lambda_o$ is the porosity calculated for the material sampled, and $\lambda_{inf}$ is the final porosity related to a certain time in the simulations. Similarly, the ratio between the fines content of the sampled material and the fines content at a certain defined time can serve as a measure of relative fines content. Average values of relative saturation (with $\lambda_R = 0{\cdot}45$, considering the maximum random loose packing of spheres) and relative fines content, obtained by comparing the initial and final conditions in simulations, are shown in the last two columns of Table 3. Again, there is a positive correspondence between these two parameters and the initial fine sediment fraction. The relative saturation for riffles and the recirculation zone would be quite similar, with less than 2% difference between the two. Conversely, the shear zone would be 5% less saturated, and would contain *ca* 10% less relative content of fines than the other two zones, on average. These results are related to the lower content of fines of samples in the shear zone, and (particularly when the coarse samples are compared in all three zones) to the number of fine size classes with a relative frequency different from zero, which is larger for the riffles and recirculation zones than for the shear zone. Such size fractions participate in the aggregation of infilling fines in simulations, which favours fast achievement of stability. In this regard, the times required to achieve stability in the simulations were approximately 60% lower on average

**Table 3.** Average results of applying the new method to field data collected by Evans & Wilcox (2014)

| Zone | Average original fine sediment fraction ($D$ <2 mm) | Average computed initial porosity $\lambda\|^{t\,=\,0}$ | Average computed final porosity $\lambda\|^{t\,=\,t_{SAT}}$ | Average computed relative saturation $\frac{(0{\cdot}45-\lambda\|^{t\,=\,0})}{(0{\cdot}45-\lambda\|^{t\,=\,t_{SAT}})}$ | Average computed relative fines content $\frac{F^{t\,=\,0}_{D<2mm}}{F^{t=t_{SAT}}_{D<2mm}}$ |
|---|---|---|---|---|---|
| Recirculation | 0·16 | 0·211 | 0·131 | 0·75 | 0·68 |
| Riffles | 0·11 | 0·220 | 0·135 | 0·73 | 0·67 |
| Shear | 0·07 | 0·253 | 0·164 | 0·69 | 0·56 |

for the riffles and recirculation zones than for the shear zone.

## DISCUSSION

The method presented in this article, to forecast the size gradation and porosity of saturated beds with fines, employs the packing porosity model of Yu & Standish (1991) for multifractional mixtures. Here, the model was used to identify three limiting geometrical conditions that the present authors suggest would constrain infiltration, namely, random close packing, filled gravel and cut-off size. For the first condition, the new approach assumes that the densest sediment packing attained by infiltration of fines would be equivalent to the random close packing state estimated by packing models. Such an assumption would be reasonable, particularly for saturation near the bed surface due to bridging, i.e. when a seal made of fines is formed. Turbulent bursts and gravel framework vibrations, generated by increments in bed shear stresses lower than the critical incipient motion condition, can optimize the packing of bed particles in superficial layers (Schälchli, 1992, 1995). Turbulent bursts and framework vibrations would resemble the shaking and tapping induced in experimental mixtures used to produce random close packing data from which empirical packing porosity models are normally calibrated (Middleton *et al.*, 2000). Although less disturbing, turbulent pressure fluctuations into the bed (Vollmer & Kleinhans, 2007) may also collapse bridges leading to deeper filling. Conversely, for bed saturation developed from deep layers up, i.e. unimpeded static percolation, it is less likely that packing of particles would be optimized by the flow action. In consequence, it can be expected that the matrix of infiltrating fines would be looser in comparison to shallow seals, that is, layers saturated by unimpeded static percolation would depart from the assumption of random close packing, so that the new method might overestimate the amount of percolated fines and underestimate the final porosity.

Simulations with experimental data showed that saturation would be related to random close packing limitations if the bed is tightly to slightly loosely packed at the initial state. For this condition, small variations in the initial bed porosity would result in large variations in the final content of infiltrated fines; for the most extreme case in simulations, increments of only 1% in the initial bed porosity used resulted in increments of saturation fines content as high as 16%. If the bed is loosely packed, the initial porosity is less important, and saturation occurs due to filled gravel or cut-off size limitations. The filled gravel state was defined as the fines content value for which packing porosity models describe a minimum porosity for the combination of a coarse mixture with fines. In turn, the cut-off size restriction was established to occur when the minimum size of particles that form the bed structure is smaller than any of the supplied grain-size fractions. Since the method simulates infiltration by aggregating small volumetric increments of sediment smaller than the bed cut-off size, it would be reasonable to consider that when filled gravel occurs, the pore openings are smaller than the size of the constituent particles of the mixture. Thus, filled gravel and the cut-off size limitation would refer to equivalent definitions of an ultimate state for the bed structure, if size fractions of the supplied material are represented in the bed. Additional simulations were performed to test the effect on final saturation conditions of neglecting either filled gravel or cut-off size restrictions. The difference in saturation porosity and fines content between filled gravel and cut-off size restrictions was lower than 3%. Hence, by using the Yu & Standish model, the almost equivalence of filled gravel and cut-off size restrictions is verified.

For the use of the Yu & Standish model, more empirical evidence is needed to draw general conclusions about appropriate values of the required parameters for porosity and cut-off size computations. Meanwhile, consistent results have been obtained by computing the cut-off size using as an initial uniform porosity the value for random close packing of hard uniform spheres, and the critical size ratio for tetrahedral packing.

An underlying hypothesis of the method is that the bed framework remains unaltered during the percolation process, a condition that is true if the coarse bed is not mobile. The method considers that packing density continuously increases as the bed is filled with fines. Hence, saturation would be related to a very densely packed arrangement of the sediment mixture, as is normally evidenced in clogged beds by low permeability values (e.g. Blaschke *et al.*, 2003). Nevertheless, if the bed is mobile, the flow may wash the fines with the entrainment or rearrangement of coarse particles, and the

assumption of a regular decrease in porosity would no longer be valid. In addition, under flow conditions close to the incipient motion of the coarse bed, during or after the formation of a low porosity deposit with infilling fines, the bed material may be prone to dilation (e.g. Frostick *et al.*, 1984; Middleton *et al.*, 2000). Allan & Frostick (1999) showed that bed dilation produces an expansion in pore throats, which may result in a rearrangement of particles and the ingress of fine grains into the bed. During experiments, Gibson *et al.* (2011) observed that as much as 20% of the total infiltrated fines may have penetrated the bed even after the formation of a bridge layer that plugged the interstitial pathways near the bed surface, or after saturation was achieved by filling the bed from below. Accordingly, bed porosity might not necessarily be irreversible during pore-filling: as the sediment fills the pores, porosity may not exhibit a monotonically decreasing path and, in that case, the initial hypothesis of an unaltered bed framework might not be valid. More experimental evidence is required to relate these processes to the properties of the flow field. Furthermore, it is not well-known to what degree the turbulent pressure fluctuations into the bed depend on the degree of filling of the pores by fines, but the present authors hypothesize that these decrease. A consequence could be that there is a threshold filling value for a given mixture below which turbulence is strong enough to entrain fines but, once exceeded, would lead to progressive filling as turbulent pressure fluctuations are dampened by the fines. These complications notwithstanding, dilation and secondary infiltration could be included in the model by introducing instantaneous increments of bed porosity, related to the displacement and rearrangement of the most superficial particles due to, for instance, turbulent bursts or the motion of coarse grains.

The application of the new method here to the field data collected by Evans & Wilcox (2014) has shown that the method can serve as a quantitative tool to estimate the degree of siltation among local sites in deposition settings, or to assess the overall degree of saturation and likely extreme scenarios and timescales. Irrespective of whether the sediment collected by Evans & Wilcox (2014) was likely to have been reworked by the flow, and the packing from likely infiltrated fines was altered, the new method was able to consider the grain-size gradation of the material collected as an initial condition to assess the capacity of the bed to be further filled with fines.

## CONCLUSIONS

In this article, a new method has been presented to estimate the saturation fines content and decrease in porosity due to progressive sediment infiltration in unconsolidated gravel frameworks. The method uses the packing porosity model of Yu & Standish (1991) to define the saturation conditions, and only requires the grain-size distributions of the bed and of the infiltrating sediment as input data. Thus, it can be concluded that:

1. The new method can be applied to any arbitrary number of size fractions because: (i) the equations were derived to generalize to sediment mixtures the original theory of fines infiltration presented by Cui *et al.* (2008); and (ii) size fractions that are small enough to ingress into the bed can be identified using an adapted version of the Yu & Standish (1991) model presented by Frings *et al.* (2008).
2. The method assumes that saturation may be restricted either by: (i) the relative size of fines with respect to the bed pores; (ii) the complete infilling of pores with fines; or (iii) random close packing of the sediment mixture. Due to this latter assumption, the present authors expect that the method would provide best results for saturation in seals close to the bed surface, rather than for saturation related to unimpeded static percolation, because flow effects can optimize bed packing near the bed surface.
3. The saturation content of infiltrated fines is strongly sensitive to the initial bed porosity, if the bed is tightly to slightly loosely packed in the initial state. These results highlight the need to measure and understand openwork gravel deposits.
4. The method performed well with published experimental data when simulated porosities and the grain sizes of infiltrated fines were compared. This notwithstanding, more empirical data are required to determine the value of the critical size ratio for infiltration and the initial porosities, to be used in the Yu & Standish (1991) model for different packing conditions of natural sediment.
5. An example of a likely practical application of the method was presented. By defining

two relations for the degree of saturation (the relation between the initial and saturated bed porosities, subtracted from a reference porosity value; and the relation between the initial and saturated fines content), it was shown that the new approach can serve as a practical tool for quantitative assessment of the degree of bed saturation with fines.

## ACKNOWLEDGEMENTS

The code for computations of cut-off size and porosity using the Yu & Standish (1991) packing porosity model was the same Matlab code as that used by Frings *et al.* (2008). Seminal ideas for this study were developed during PhD research by the first author, supported partly by the Programme Alβan, No. (E04D048796MX) and partly by Conacyt, México (179047). The first author would like to thank Bernd Ettmer, at the Hochschule Magdeburg-Stendal, for the institution's financial support. Three anonymous reviewers provided many helpful comments that greatly improved this manuscript as well as the conclusions of the study. The Matlab code used in this study is available on request.

## NOTATIONS

| | |
|---|---|
| $C_i$ | Fractional content by volume of the *i*th grain size |
| $D$, $d$ | Grain size of the bed and the pore-filling sediment, respectively |
| $D_c$ | Cut-off size for grains smaller than pore spaces in the bed |
| $D_{c\ FYS}$ | Denotes computations with the method for estimating the cut-off size of a sediment mixture, developed by Frings *et al.* (2008) using the original method of Yu & Standish (1988, 1991) |
| $D_g$ | Geometrical mean diameter of a mixture of coarse particles |
| $D_m$, $d_m$ | Geometrical mean diameter of coarse bed and infiltrating material, respectively |
| $D_x$, $d_x$ | Grain size for which $x$% of the particles in the sample are smaller, in coarse bed material and fine infilling sediment, respectively |
| $F_f$ | Fractional content by weight of infiltrated fines in bed |
| $F_i$ | Fractional content by weight of the *i*th size class in bed |
| $f_D$, $f_d$ | Relative proportion of coarse and fine particles $D$ and $d$, respectively, in a mixture |
| $f_{dSAT}$ | Relative proportion of fine particles in a saturated mixture |
| $f_{d_{SAT(FG)}}$ | Relative proportion of fine particles in a mixture saturated due to filled gravel restrictions |
| $f_{d_{SAT(RCP)}}$ | Relative proportion of fine particles in a mixture saturated due to random close packing restrictions |
| $f_i$ | Fractional content by weight of the *i*th size class in sediment flux |
| $i$ | *i*th grain-size fraction |
| $j$ | *j*th packing arrangement of a given mixture |
| $N$ | *N*th size class limit |
| $n$ | Number of size fractions |
| $q_T$ | Total downward sediment flux per unit area |
| $q_i$ | Downward sediment flux for *i*th size fraction per unit area |
| $r$ | Size ratio between fine and coarse particles |
| $r_d$ | Critical size ratio between small and large particles that still allows the small particles to fit in the pores of the larger particles |
| $SAT$ | Subscript to indicate conditions in the saturated stable state of infiltration |
| $t$ | Time |
| $z$ | Downward vertical coordinate |
| $\alpha$ | Ratio between the mass volume entering into the bed every time step, to the volume-space in the finite volume |
| $\Delta t$ | Increment of time |
| $\Delta z$ | Thickness of a finite volume in the bed substrate |
| $\lambda$ | Bed porosity |
| $\lambda_D$, $\lambda_d$ | Pure porosity of large and small particles $D$ and $d$, respectively, in a stack of identical elements |
| $\lambda_{YS}$ | Functional relation solved by the algorithm to compute packing porosity with the Yu & Standish model |
| $\lambda_{PM}$ | Functional relation solved by a packing porosity model to estimate porosity |
| $\lambda_{RCP}$, $\lambda_{RLP}$ | Porosity related to random close packing and random loose packing, respectively |
| $\lambda_{inf}$ | Bed porosity at a given stage of the infiltration of a fine mixture |

| | |
|---|---|
| $\lambda_R$ | Reference porosity to calculate relative saturation |
| $\lambda_o$ | Initial bed porosity at the beginning of infiltration |
| $\lambda_u$ | Initial porosity associated with uniform material, for mixture porosity computations |
| $\lambda_{u(min)}$, $\lambda_{u(max)}$ | Initial porosity associated with uniform material related to minimum random close packing and maximum random loose packing, respectively |
| $\sigma_c$ | Geometric standard deviation of coarse particles in a mixture |
| $\sigma_g$ | Geometric standard deviation |

## REFERENCES


**Alberts, L.J.H.** (2005) *Initial Porosity of Random Packing. Computer Simulation of Grain Rearrangement*. Thesis, Department of Geotechnology, Delft University of Technology, 136 pp.

**Allan, A.F.** and **Frostick, L.** (1999) Framework dilation, winnowing, and matrix particle size: the behavior of some sand-gravel mixtures in a laboratory flume. *J. Sed. Res.*, **69**, 21–26.

**Beschta, R.L.** and **Jackson, W.L.** (1979) The intrusion of fine sediments in a stable gravel bed. *J. Fish. Res. Board Can.*, **36**, 204–210.

**Blaschke, A.P.**, **Steiner, K.**, **Schmalfuss, R.**, **Gutknecht, D.** and **Sengschmitt, D.** (2003) Clogging processes in hyporheic interstices of an impounded river, the Danube at Vienna, Austria. *Int. Rev. Hydrobiol.*, **88**, 397–413.

**Brunke, M.** (1999) Colmation and depth filtration within streambeds: retention of particles in hyporheic interstices. *Int. Rev. Hydrobiol.*, **84**, 99–117.

**Carling, P.A.** (1984) Deposition of fine and coarse sand in an open-work bed. *Can. J. Fish Aquat. Sci.*, **41**, 263–270.

**Carling, P.A.** and **Gleister, M.S.** (1987) Rapid deposition of sand and gravel mixtures downstream of a negative step: the role of matrix-infilling and particle-overpassing in the process of bar-front accretion. *J. Geol. Soc.*, **144**, 543–551.

**Chapman, D.W.** (1988) Critical review of variables used to define effects of fines in redds of large salmonids. *Trans. Am. Fish. Soc.*, **117**, 1–21.

**Church, M.A.**, **McLean, D.G.** and **Wolcott, J.F.** (1987) River bed gravels: sampling and analysis. In: *Sediment Transport in Gravel-bed Rivers* (Eds C.R. Thorne, J.C. Bathurst and R.D. Hey), pp. 43–88. John Wiley & Sons Ltd., New York.

**Coulombe-Pontbrianda, M.** and **Lapointe, M.** (2004) Geomorphic controls, riffle substrate quality, and spawning site selection in two semi-alluvial salmon rivers in the Gaspé Peninsula, Canada. *River Res. Applic.*, **20**, 577–590.

**Cui, Y.**, **Wooster, J.K.**, **Baker, P.F.**, **Dusterhoff, S.R.**, **Sklar, L.S.** and **Dietrich, W.E.** (2008) Theory of fine sediment infiltration into immobile gravel bed. *J. Hydraul. Eng.*, **134**, 1421–1429.

**Denic, M.** and **Geist, J.** (2015) Linking stream sediment deposition and aquatic habitat quality in pearl mussel streams: implications for conservation. *River Res. Applic.*, **31**, 943–952.

**Dias, R.P.**, **Teixeira, J.A.**, **Mota, M.G.** and **Yelshin, A.I.** (2004) Particulate binary mixtures: dependence of packing porosity on particle size ratio. *Ind. Eng. Chem. Res.*, **43**, 7912–7919.

**Diplas, P.** and **Parker, G.** (1992) Deposition and removal of fines in gravel-bed streams. In: *Dynamics of Gravel-Bed Rivers* (Eds P. Billi, R.D. Hey, C.R. Thorne and P. Tacconi), pp. 313–329. Wiley, Chichester, UK.

**Einstein, H.A.** (1968) Deposition of suspended particles in a gravel bed. *J. Hydraul. Div. ASCE*, **94**, 1197–1205.

**Evans, E.** and **Wilcox, A.C.** (2014) Fine sediment infiltration dynamics in a gravel-bed river following a sediment pulse. *River Res. Applic.*, **30**, 372–384. doi:10.1002/rra.2647.

**Ferrer-Boix, C.** and **Hassan, M.** (2014) Influence of the sediment supply texture on morphological adjustments in gravel-bed rivers'. *Water Resour. Res.*, **50**, 8868–8890.

**Finkers, H.J.** and **Hoffmann, A.C.** (1998) Structural ratio for predicting the voidage of binary particle mixtures. *AIChE J.*, **44**, 495–498.

**Frings, R.**, **Kleinhans, M.** and **Vollmer, S.** (2008) Discriminating between pore-filling load and bed-structure load: a new porosity-based method, exemplified for the river Rhine. *Sedimentology*, **55**, 1571–1593. doi:10.1111/j.1365-3091.2008.00958.x.

**Frings, R.M.**, **Schüttrumpf, H.** and **Vollmer, S.** (2011) Verification of porosity predictors for fluvial sand-gravel deposits. *Water Resour. Res.*, **47**, 1–15. doi:10.1029/2010WR009690.

**Frostick, L.**, **Lucas, P.M.** and **Reid, I.** (1984) The infiltration of fine matrices into coarse-grained alluvial sediments and its implications for stratigraphical interpretation. *J. Geophys. Soc.*, **141**, 955–965.

**Gayraud, S.** and **Philippe, M.** (2003) Influence of bed-sediment features on the interstitial habitat available for macroinvertebrates in 15 french streams. *Int. Rev. Hydrobiol.*, **88**, 77–93.

**Gibson, S.**, **Abraham, D.**, **Heath, R.** and **Schoellhamer, D.** (2009) Vertical gradational variability of fines deposited in a gravel framework. *Sedimentology*, **56**, 661–676. doi:10.1111/j.1365-3091.2008.00991.x.

**Gibson, S.**, **Abraham, D.**, **Heath, R.** and **Schoellhamer, D.** (2010) Bridging process threshold for sediment infiltrating into a coarse substrate. *ASCE J. Geotech. Geoenviron. Eng.*, **136**, 402–406.

**Gibson, S.**, **Heath, R.**, **Abraham, D.** and **Schoellhamer, D.** (2011) Visualization and analysis of temporal trends of sand infiltration into a gravel bed. *Water Resour. Res.*, **47**, 11. doi:10.1029/2011WR010486.

**Hodge, R.A.**, **Sear, D.A.** and **Leyland, J.** (2013) Spatial variations in surface sediment structure in riffle–pool sequences: a preliminary test of the Differential Sediment Entrainment Hypothesis (DSEH). *Earth Surf. Proc. Land.*, **38**, 449–465. doi:10.1002/esp.3290.

**Iseya, F.** and **Ikeda, H.** (1987) Pulsations in bedload transport rates induced by a longitudinal sediment sorting: a flume study using sand and gravel mixtures. *Geogr. Ann. Ser. A*, **69**, 15–27.

**Julien, H.P.** and **Bergeron, N.E.** (2006) Effect of fine sediment infiltration during the incubation period on Atlantic salmon (*Salmo salar*) embryo survival. *Hydrobiologia*, **563**, 61–71.

**Kleinhans, M.G.** (2002) *Sorting Out Sand and Gravel: Sediment Transport and Deposition in Sand-Gravel Bed Rivers*. PhD Thesis. Netherlands Geographical Studies 293, The Royal Dutch Geographical Society/Faculty of Geographical Sciences, Utrecht University.

**Koltermann, C.E.** and **Gorelick, S.M.** (1995) Fractional packing model for hydraulic conductivity derived from sediment mixtures. *Water Resour. Res.*, **31**, 3283–3297.

**Lauck, T.** (1991) *A Simulation Model for the Infiltration of Sediment Into a Spawning Gravel*. MS Thesis. Humboldt State University, Arcata, CA.

**Lisle, T.E.** (1989) Sediment transport and resulting deposition in spawning gravels, North Coastal California. *Water Resour. Res.*, **25**, 1303–1319.

**Liu, S.** and **Ha, Z.** (2002) Prediction of random packing limit for multimodal particle mixtures. *Powder Technol.*, **126**, 283–296.

**McGeary, R.** (1961) Mechanical packing of spherical particles. *J. Am. Ceram. Soc.*, **44**, 513–522.

**Middleton, R.**, **Brasington, J.**, **Murphy, B.J.** and **Frostick, L.E.** (2000) Monitoring gravel framework dilation using a new digital particle tracking method. *Comput. Geosci.*, **26**, 329–340.

**Onoda, G.Y.** and **Liniger, E.G.** (1990) Random loose packings of uniform spheres and the dilatancy onset. *Phys. Rev. Lett.*, **64**, 2727–2730.

**Peterson, R.H.** (1978) *Physical Characteristics of Atlantic Salmon Spawning Gravel in Some New Brunswick Streams*. Fisheries and Marine Service, Technical Report No. 785. Fisheries and Oceans Canada Biology Station, St. Andrews, New Brunswick.

**Rehg, K.J.**, **Packman, A.I.** and **Ren, J.** (2005) Effects of suspended sediment characteristics and bed sediment transport on streambed clogging. *Hydrol. Process.*, **19**, 413–427.

**Sakthivadivel, R.** and **Einstein, H.A.** (1970) Clogging of porous column of spheres by sediment. *Hydraul. Div. Am. Soc. Civ. Eng.*, **94**, 1197–1205.

**Sambrook Smith, G.H.** and **Nicholas, A.P.** (2005) Effect on flow structure of sand deposition on a gravel bed: results from a two-dimensional flume experiment. *Water Resour. Res.*, **41**, W10405. doi:10.1029/2004WR003817.

**Schälchli, U.** (1992) The clogging of coarse gravel river beds by fine sediment. *Hydrobiologia*, **235–236**, 189–197.

**Schälchli, U.** (1995) Basic equations for siltation of riverbeds. *J. Hydraul. Eng.*, **121**, 274–287.

**Scott, G.D.** and **Kilgour, D.M.** (1969) The density of random close packing of spheres. *J. Phys. D.*, **2**, 863–866.

**Smith, N.D.** (1974) Sedimentology and bar formation in the upper Kicking Horse River: a braided meltwater stream. *J. Geol.*, **82**, 205–223.

**Soppe, W.** (1990) Computer simulation of random packings of hard spheres. *Powder Technol.*, **62**, 189–196.

**Viparelli, E.**, **Sequeiros, O.E.**, **Cantelli, A.**, **Wilcock, P.R.** and **Parker, G.** (2010) River morphodynamics with creation/consumption of grain size stratigraphy 2: numerical model. *J. Hydraul. Res.*, **48**, 727–741.

**Vollmer, S.** and **Kleinhans, M.G.** (2007) Predicting incipient motion, including the effect of turbulent pressure fluctuations in the bed. *Water Resour. Res.*, **43**, W05410. doi:10.1029/2006WR004919.

**Westman, A.** (1936) The packing of particles empirical equations for intermediate diameter ratios. *J. Am. Ceram. Soc.*, **19**, 127–129.

**Wilcock, P.R.** (2001) Toward a practical method for estimating sediment-transport rates in gravel-bed rivers. *Earth Surf. Proc. Land.*, **26**, 1395–1408.

**Wilcock, P.R.** and **Kenworthy, S.T.** (2002) A two-fraction model for the transport of sand/gravel mixtures. *Water Resour. Res.*, **38**, 1194.

**Wooster, J.K.**, **Dusterhoff, S.R.**, **Cui, Y.**, **Sklar, L.S.**, **Dietrich, W.E.** and **Malko, M.** (2008) Sediment supply and relative size distribution effects on fine sediment infiltration into immobile gravels. *Water Resour. Res.*, **44**, 18. doi:10.1029/2006WR005815.

**Wu, F.** and **Huang, H.** (2000) Hydraulic resistance induced by deposition of sediment in porous medium. *J. Hydraul. Eng.*, **126**, 547–551.

**Yu, A.B.** and **Standish, N.** (1988) An analytical-parametric theory of the random packing of particles. *Powder Technol.*, **55**, 171–186.

**Yu, A.B.** and **Standish, N.** (1991) Estimation of the porosity of particle mixtures by a linear-mixture packing model. *Ind. Eng. Chem. Res.*, **30**, 1372–1385.

*Manuscript received 19 March 2015; revision accepted 7 December 2015*

## APPENDIX A

### Westman Porosity Model

The Westman (1936) empirical model for predicting the voidage of binary particle mixtures is given by the equation:

$$\left(\frac{V - V_D f_D}{V_d}\right)^2 + 2G\left(\frac{V - V_D f_D}{V_d}\right)\left(\frac{V - f_D - V_d f_d}{V_d - 1}\right) + \left(\frac{V - f_D - V_d f_d}{V_d - 1}\right)^2 = 1 \quad \text{(A1)}$$

where $G$ is a fitting parameter; $V$ is the specific volume calculated from $1/(1 - \lambda)$, with $\lambda$ being the porosity of the mixture; $V_D$ and $V_d$ are the specific volumes for large and small particles, respectively, calculated with the porosities $\lambda_D$ and $\lambda_d$ of beds of the pure particle fractions; $f$ is the volume fraction and the subscripts $D$ and $d$ refer to large and small particles, respectively.

For spherical and non-spherical particles, Finkers & Hoffmann (1998) calculated $G$ as:

$$G = r_{str}^{k} + (1 - \lambda_D^{-k}) \quad \text{(A2)}$$

where $k$ is a constant, which empirically was found to take the value $-0{\cdot}63$ for monosized particles or those with a narrow size distribution, and $-0{\cdot}345$ for particles with a wider size distribution; $r_{str}$ is the structural ratio, i.e. the ratio of the volume of a small particle with its associated interstitial region to the volume of the interstitial region associated with a large particle, calculated from:

$$r_{str} = \frac{\left(\frac{1}{\lambda_D} - 1\right) r^3}{1 - \lambda_d} \quad \text{(A3)}$$

where $r$ is the size ratio, i.e. $r = d/D$.